CQE Center for Quantitative Economics

Extracting stock-market bubbles from dividend futures

Nicole Branger[#], Mark Trede[†], Bernd Wilfling[†]

107/2024

[#] Finance Center, University of Münster, Germany
[†] Department of Economics, University of Münster, Germany

wissen.leben
Universität Münster

Extracting stock-market bubbles from dividend futures

Nicole Branger [a], Mark Trede [b], Bernd Wilfling [b*]

[a] *Universität Münster, Finance Center (FCM), Universitätsstraße 14-16, 48143 Münster, Germany*

[b] *Universität Münster, Department of Economics (CQE), Am Stadtgraben 9, 48143 Münster, Germany*

(Date of this version: August 27, 2024)

Abstract

This study presents a method for decomposing the EuroStoxx50 index into its unobservable bubble and its fundamental component. Based on a unique data set containing the prices of dividend futures from 2011 to 2023, we determine the fundamental value by extrapolating the price curve of dividend claims for long maturities. As a residual, we obtain the trajectory of the bubble. We find that the bubble component averages around 22% of the EuroStoxx50 index in normal times. The bubble is highly sensitive to increasing geopolitical risks and economic uncertainty triggered by the invasion of Ukraine and the COVID19 outbreak. Our econometric analysis indicates that the fitted bubble process is consistent with rational expectations.

Keywords: Rational bubbles; Present-value model; Dividend futures; Equity yields; Explosive behavior.

JEL classification: C1, C22, E44, G12, G13.

*Corresponding author. Tel.: +49 251 83 25040; fax: +49 251 83 25042.
E-mail addresses: nicole.branger@wiwi.uni-muenster.de (N. Branger), mark.trede@uni-muenster.de (M. Trede), bernd.wilfling@wiwi.uni-muenster.de (B. Wilfling).

1 Introduction

Owing to their impact on financial markets and the real economy, stock-market bubbles have always attracted considerable attention in the economics, finance, and econometrics literature. A plethora of theoretical and empirical articles study the emergence of asset-price bubbles and the behavior of agents during bubbly periods, including, among others, Tirole (1982, 1985), Allen and Gorton (1993), Allen and Gale (2000) , Abreu and Brunnermeier (2003), Barberis et al. (2018), Bordalo et al. (2021), Enders and Hakenes (2021), Braggion et al. (2023). In this paper, we focus on the following two strands of the literature. The first consists of econometric studies that are concerned with the empirical detection, date-stamping and monitoring of bubbles in artificial and real-world financial data, predominantly by applying cointegration-, unit-root-, and explosivity tests to a dividend-stock-price relationship (*inter alia*, Diba and Grossman, 1988a; Hall et al., 1999; Phillips et al., 2011; Homm and Breitung, 2012; Phillips et al., 2015; Shi and Song, 2016; Hafner, 2018; Harvey et al., 2020; Kurozumi, 2020; Monschang and Wilfling, 2021; Caravello et al., 2023; Morita et al., 2023; Lui et al., 2024; Blasques et al., 2024). The second strand includes articles that aim to disentangle the latent bubble process from other financial/economic variables and characteristics (usually summarized as fundamentals). Surprisingly, relatively few attempts have so far been undertaken in this latter direction, e.g. Wu (1995), Wu (1997), Balke and Wohar (2009), Al-Anaswah and Wilfling (2011), Lammerding et al. (2013), Rotermann and Wilfling (2014), Chan and Santi (2021). The results of our study primarily contribute to this area.

Several of the latter articles use specific variants of the log-linearized present-value model with time-varying expected returns (Campbell and Shiller, 1988a, 1988b; Engsted et al., 2012). The econometric setup consists of three unobservable variables, namely (i) the expected stock returns, (ii) the expected dividends, and (iii) the bubble values, whose dynamics are specified in the transition equation of a state-space representation (e.g. Balke and Wohar, 2009; Chan and Santi, 2021). The three latent processes are assumed to follow low-order autoregressive patterns, in which the bubble process is sometimes enriched with two-regime Markov-switching elements to take account of exploding and collapsing bubble phases. Along with the process specifications of the observable model variables in the measurement equation, the entire state-space framework is then estimated by maximum-likelihood or Bayesian techniques, ultimately yielding an estimate of the bubble process.

Given the limited availability of past data, this well-designed state-space framework provides a compelling method for drawing inferences about the nature of unobservable stock price bubbles. One aspect regarding the estimation of the bubble process with this state-space technique, however, is worth mentioning. Since the latent expected dividend and return processes must be estimated from the data, the final estimates of the bubble process may be exposed to potential (i) misspecifcation of the dividend and return equations, and (ii) es-

timation errors within the state-space system. In the following analysis, we circumvent such econometric pitfalls by using a novel and comprehensive data base that allows a more direct extraction of bubble values (without estimation).

Our data sets include time series of EuroStoxx dividend-futures prices over the next 10 years, which have been available since 2008 for expiry dates from 2008 to 2032. The underlying of a dividend future for a given year is the sum of the dividends paid over the course of that year. For instance, the dividend-futures contract for 2025 entitles the holder to receive the dividends paid in 2025 in the middle of December 2025. Additionally, we use spot interest-rate data from the European Central Bank (ECB) to obtain risk-free rates for given maturities. These two time series enable us to recover the fundamental value of the EuroStoxx in a basically model-free way. The main idea is that the fundamental value is the sum over the prices of all dividend claims. For a maturity of 1 to 10 years, we can recover the prices of these dividend claims from the prices of the corresponding dividend futures. For maturities of 11 years onwards (to infinity), we extrapolate the price curve of the dividend claims, more specifcally, the curve of the forward equity yields. The difference between the EuroStoxx and its fundamental value is then, by definition, equal to the value of the bubble. Having revealed the entire bubble trajectory via this procedure, we are then able (i) to analyze the statistical properties of the disentangled fundamental and bubble values, and (ii) to fit suitable theoretical (parametric) bubble process specifications directly to the extracted bubble trajectory.

Our data-driven approach is based on minimal assumptions only. The crucial point involves our choice of the exponential function, which we use for the above-mentioned extrapolation. To justify our functional form, we determine the prices of dividend claims and the equity yields in an equilibrium model. Specifically, we rely on the long-run risk model of Bansal and Yaron (2004) with a stochastic expected growth rate of consumption and stochastic volatility. The theoretical analysis yields three major findings. (i) The model-implied equity yield curve is well fitted by the exponential function. (ii) The assumed behavior of the dividend claims and the forward equity yield curves is in line with their properties in this long-run risk model. (iii) Using the parameters of Bansal et al. (2016), we obtain a long-run level of the forward equity yield of around 7.5% with an approximately exponential convergence to this level. Slight variations in the parameters in particular in the mean-reversion speed of the expected growth rate yield long-run levels for the forward equity yield between 2% and 12%, suggesting that our data-driven choice of a long-run level of around 11% is sensitive.

The last element we need is a suitable theoretical (parametric) bubble process that we can fit to our bubble values. In the literature, several bubble specifications have been motivated within the linear present-value model under rational expectations and with a constant discount factor (e.g. Evans, 1991; Fukuta, 1998; Rotermann and Wilfling, 2018). However, Cochrane (2011) presents overwhelming empirical significance of time-varying dis-

count rates and vigorously advocates the inclusion of discount-rate variation into financial and econometric modeling. In the preliminary Section 2 below, we therefore modify the conventional constant-discount-factor present-value model by relying on stochastic discount factors within a general asset-pricing framework. This leads directly to (i) the possibility of time-varying discount rates without log-linearization of the basic present value model, and (ii) a theoretical bubble process with identifiable and easily interpretable parameters (after estimation).

The four main findings of our empirical bubble and fundamental-value analysis can be summarized as follows. (i) The average bubble share in the EuroStoxx50 was around 22% in the period from January 2011 to December 2023. (ii) The bubble share and the bubble values reacted strongly to significant geopolitical events (Crimean annexation, war in Ukraine) and the outbreak of the COVID-19 pandemic. (iii) The bubble series exhibits explosiveness characteristics and martingale/random-walk behavior comparable to that of the EuroStoxx50 index. (iv) The estimation results obtained by fitting our theoretical bubble process to the data indicate that the EuroStoxx50 bubble was consistent with rational expectations.

The remainder of the paper is organized as follows. Section 2 presents our stock-price model with time-varying (stochastic) discount rates and our theoretical (parametric) bubble process. Section 3 describes the EuroStoxx dividend futures dataset. Section 4 presents the method for extracting the fundamental and bubble values from the data. The empirical Section 5 analyzes the statistical properties of the EuroStoxx bubble. Section 6 concludes.

2 Stock-price model with rational bubble

2.1 A rational bubble process

To introduce our parametric bubble specification, we briefly review the linear present-value model with constant expected returns (Campbell et al., 1997; Cuthbertson and Nitzsche, 2004), in which the price of a stock at date t, P_t, is given by the Euler equation

$$P_t = \mathbb{E}_t\left[\frac{1}{1+r}\left(P_{t+1} + D_{t+1}\right)\right] = \frac{1}{1+r}\left[\mathbb{E}_t(P_{t+1}) + \mathbb{E}_t(D_{t+1})\right]. \tag{1}$$

$\mathbb{E}_t(\cdot)$ denotes the conditional expectation operator based on all information available to market participants at time t, D_{t+1} is the dividend payment of the stock between t and $t+1$, and r is referred to as the *required rate of return* that is just sufficient to compensate investors for the inherent riskiness of the stock. The first-order expectational difference equation (1) can be solved routinely. If we rule out bubble solutions by imposing the transversality condition

$$\lim_{n\to\infty}\left(\frac{1}{1+r}\right)^n \cdot \mathbb{E}_t(P_{t+n}) = 0, \tag{2}$$

the Euler equation (1) has the unique solution

$$P_t = P_t^f \equiv \sum_{i=1}^{\infty} \left(\frac{1}{1+r} \right)^i \cdot \mathbb{E}_t(D_{t+i}). \tag{3}$$

In Eq. (3), P_t^f is the fundamental stock-price (the stream of discounted expected future dividends).

Relaxing the transversality condition (2), we obtain an entire class of solutions to Eq. (1), which can be written as

$$P_t = P_t^f + B_t = \sum_{i=1}^{\infty} \left(\frac{1}{1+r} \right)^i \cdot \mathbb{E}_t(D_{t+i}) + B_t, \tag{4}$$

where B_t in Eq. (4) may be any stochastic process satisfying the submartingale property

$$\mathbb{E}_t(B_{t+1}) = (1+r) \cdot B_t \qquad \text{or, equivalently,} \qquad B_t = \frac{1}{1+r} \cdot \mathbb{E}_t(B_{t+1}). \tag{5}$$

Any process $\{B_t\}$, satisfying Property (5), is called a rational bubble, since its presence in Eq. (4) is consistent with rational expectations.

Besides the submartingale property (5), any rational bubble with respect to an asset with limited liability has to meet two additional formal properties, as argued by Diba and Grossman (1988b): (i) rational bubbles cannot start from zero, and (ii) negative bubbles are ruled out as $t \to \infty$. The most frequently applied rational bubble, satisfying both Diba-Grossman conditions, is the periodically collapsing Evans (1991) process. An empirical shortcoming of the Evans bubble is that it always bursts completely from one trading unit to the next, implying unrealistic (theoretical) stock-price volatility paths (Rotermann and Wilfling, 2014).

Rotermann and Wilfling (2018) propose a flexible bubble specification that generates stock prices and (time-varying) stock-price variances with more realistic deflating behavior.[1] To formalize, let $\{u_t\}_{t=1}^{\infty}$ be an exogenous process of i.i.d. lognormally (LN) distributed random variables, for which each variable is scaled to have unit mean.[2] Then, the Rotermann and Wilfling (2018) bubble (RW bubble) is defined as the following mixture of two lognormal distributions:

$$B_{t+1} = \begin{cases} \frac{1}{\psi}\frac{\alpha}{\pi} B_t u_t & , \text{ with probability } \pi \\ \frac{1}{\psi}\frac{1-\alpha}{(1-\pi)} B_t u_t & , \text{ with probability } 1-\pi \end{cases}, \tag{6}$$

with parameters $\psi \equiv (1+r)^{-1}, \alpha$, and π, for which it is assumed that $0 < \alpha < 1, \frac{\alpha}{\pi} > 1$, and $\frac{1-\alpha}{1-\pi} < \psi$. Under these restrictions, the process (6) is interpreted as follows. In State 1

[1] Fukuta (1998) defines an incompletely bursting bubble, which evolves over time along three potential states ('large-bubble', 'small-bubble', 'incomplete-burst' state). However, within each state, the Fukuta bubble exhibits deterministic growth, a property which frequently conflicts with empirical findings.

[2] Technically, we assume $u_t \overset{\text{i.i.d.}}{\sim} \text{LN}(\frac{-\iota^2}{2}, \iota^2)$.

(occurring with probability π), the bubble grows at the expected rate $\frac{\alpha}{\psi\pi} - 1 > r$. In this state, the bubble grows at a faster rate than the required rate of return. In State 2 (occurring with probability $1-\pi$), the expected bubble growth rate is $\frac{1-\alpha}{\psi(1-\pi)} - 1 < 0$, i.e. in State 2, the bubble deflates.

It is straightforward to verify that the bubble-process mixture (6), (i) meets the submartingale property (5), i.e. is rational per definition, and (ii) also satisfies both Diba-Grossman conditions. In Section 2.2, we will exploit the structure of this specification to define a rational bubble in an asset-pricing framework with time-varying (stochastic) discount factors.

2.2 An asset-pricing view

We now drop the assumption of a constant expected rate of return. In line with Cochrane (2005), we assume that the stock price at date t follows the asset-pricing equation

$$P_t = \mathbb{E}_t(M_{t+1} \cdot X_{t+1}), \tag{7}$$

where M_{t+1} is the stochastic discount factor and X_{t+1} the random future payoff. By analogy with Section 2.1, we define the future payoff to consist of the components

$$X_{t+1} = P_{t+1} + D_{t+1} = P^f_{t+1} + D_{t+1} + B_{t+1} \tag{8}$$

with future fundamental value P^f_{t+1}, dividend payment D_{t+1}, and bubble term B_{t+1}. Inserting Eq. (8) into Eq. (7), we obtain

$$P_t = \mathbb{E}_t\left[M_{t+1}\left(P^f_{t+1} + D_{t+1}\right)\right] + \mathbb{E}_t\left(M_{t+1}B_{t+1}\right) = P^f_t + B_t. \tag{9}$$

The first term on the right side of Eq. (9) represents the current fundamental stock price, the second term the current bubble value. In the formula for P^f_t, we can (i) substitute out future fundamental stock prices, and (ii) exploit the economic fact that expected future fundamental stock prices cannot grow indefinitely at faster rates than the entire payoffs. This implies

$$\lim_{\tau\to\infty} \mathbb{E}_t\left(P^f_{t+\tau}\prod_{k=1}^{\tau} M_{t+k}\right) = 0,$$

which yields the following representation of the current fundamenal stock price:

$$P^f_t = \mathbb{E}_t\left(\sum_{\tau=1}^{\infty} D_{t+\tau}\prod_{k=1}^{\tau} M_{t+k}\right). \tag{10}$$

The current bubble value follows the condition $B_t = \mathbb{E}_t(M_{t+1}B_{t+1})$, which we interpret as the stochastic-discount-factor counterpart to the rationality property stated in Eq. (5). Denoting the (time-varying) risk-free interest rate at date t by r_t, we now modify the RW-bubble

specification from Eq. (6) to

$$B_{t+1} = \begin{cases} \frac{1}{\psi_t}\frac{\alpha}{\pi} B_t u_t & \text{, with probability } \pi \\ \frac{1}{\psi_t}\frac{1-\alpha}{(1-\pi)} B_t u_t & \text{, with probability } 1-\pi \end{cases}, \tag{11}$$

where $\psi_t \equiv (1 + r_t)^{-1}$.

Figure 1 about here

Figure 2 about here

3 EuroStoxx dividend-futures data

Our data set contains prices of dividend futures (maturing up to 10 years ahead), dividend point indices, and index values for the EuroStoxx50. We start depicting the data with two plots illustrating different aspects of dividend-futures prices. Figure 1 plots the prices of a dividend future with a given expiry date over time. Figure 2 shows the prices of dividend futures as a function of maturity on a specific trading day. Explicitly, data for EuroStoxx dividend futures are available since 2008 for expiry years ranging from 2008 to 2032. We denote the day-t price of the dividend future with expiry year m by $D_t^{(m)}$, so that Figure 1 shows the 25 curves (1) $\left\{D_{t_{2008}}^{(2008)}, \ldots, D_{T_{2008}}^{(2008)}\right\}$, (2) $\left\{D_{t_{2009}}^{(2009)}, \ldots, D_{T_{2009}}^{(2009)}\right\}, \ldots,$ (25) $\left\{D_{t_{2032}}^{(2032)}, \ldots, D_{T_{2032}}^{(2032)}\right\}$. The observation periods $(t_m, \ldots, T_m)$ typically differ across maturities, since each dividend future is only traded for a limited period. The panels in Figure 2 contain 16 maturity curves, for which each panel—representing a specific trading day— displays the prices of all dividend futures available on that trading day, as a function of the expiry year. For example, the upper right panel shows dividend-futures prices on 1 October 2010 (t = 2010-10-01) for the expiry years $m = 2010, 2011, \ldots, 2019$, i.e. the 10-point curve $\left\{D_t^{(2010)}, \ldots, D_t^{(2019)}\right\}$.

Figure 3 about here

Panel (a) in Figure 3 displays the dividend point index over time. Each year, the point index starts with the value 0 on the first Monday after the third Friday of December. From this day onwards, all dividend payments over the year are cumulated until the third Friday of the following December. Panel (b) shows the EuroStoxx index over the same time period, while Panels (c) and (d) are reserved for interest-rate quantities. In particular, we use spot rates calculated from ECB data for the parameters of the Svensson-approximation (available on a daily basis). The approximation is for AAA bonds only, and should thus provide accurate proxies of the risk-free interest rates. Subsequently, we denote the risk-free term-L interest rate by $r_t^{[L]}$. Panel (c) displays the time series for the 1-year risk-free rate $\left\{r_1^{[1]}, r_2^{[1]}, \ldots, r_T^{[1]}\right\}$,

while Panel (d) contains the yield curves $\left\{r_t^{[L]}\right\}$ for varying terms L (in years) on the selected days $t \in \{2007\text{-}12\text{-}31, 2019\text{-}12\text{-}30, 2023\text{-}12\text{-}01\}$.[3]

Figure 4 about here

In line with Eqs. (3) and (10), the data presented in Figures 1 to 3 constitute our quantitative basis in determining fundamental stock-price values. To extract the price $\widetilde{D}_t^{(m)}$ of the dividend claim with maturity in year m, we take the dividend futures price $D_t^{(m)}$ as an approximation of the dividend forward price, ignoring any correlation between dividend prices and interest rates. Discounting the futures price then yields the price of the dividend claim, i.e.

$$\widetilde{D}_t^{(m)} = \frac{D_t^{(m)}}{\left(1 + r_t^{[L^*]}\right)^{L^*}}, \tag{12}$$

where L^* is the number of years between day t and the expiry day of the dividend future with expiry year m. Figure 4 displays the logarithm of the prices of the dividend claims, $\ln\left[\widetilde{D}_t^{(m)}\right]$, using the maturity curves $D_t^{(m)}$ from Figure 2. In the next section, the slopes at the right end of the discounted maturity curves in Figure 4 become important,

$$s_t^{[M^*]} = \ln\left[\widetilde{D}_t^{(M)}\right] - \ln\left[\widetilde{D}_t^{(M-1)}\right], \tag{13}$$

where M is the expiry year of the longest-running dividend future at day t and M^* the associated maturity.

We can give the geometric entitity $s_t^{[M^*]}$ in Eq. (13) the following finance rationale. To determine the fundamental stock-price, we have to extrapolate the log-price curves in Figure 4. Instead of directly working with the dividend-claim price levels, we find it more convenient to express the dividend-claim prices via the forward equity yields $e_t^{[k]}$, where k refers to the period from $k-1$ to k, and then to extrapolate the forward equity yields.[4] Analogous to the forward interest rates for a bond, the forward equity yields for a stock market index follow from

$$\widetilde{D}_t^{(m)} = D_t \cdot \exp\left(-\sum_{k=1}^{m^*} e_t^{[k]}\right), \tag{14}$$

where m is the expiry year and m^* is the associated maturity. The forward equity yield $e_t^{[M^*]}$ then equals the negative slope of the log dividend price curve from Eq. (13), i.e.

$$e_t^{[M^*]} = -\left(\ln\left[\widetilde{D}_t^{(M)}\right] - \ln\left[\widetilde{D}_t^{(M-1)}\right]\right) = -s_t^{[M^*]}. \tag{15}$$

[3] From now on, we adopt the following notation: superscripts in round brackets, $(\cdot)$, denote prospective dates (such as expiry dates). Superscripts in squared brackets, $[\cdot]$, denote maturities/terms.

[4] For the definition of equity yields, see e.g. van Binsbergen et al. (2013).

Figure 5 about here

Figure 5 shows that the slopes of the longest running dividend future with maturity $M^* = 10$ years, $s_t^{[10]}$, are volatile, especially at the beginning of the observation period. Positive slopes can be ruled out according to economic theory, as they imply divergence of the fundamental value. Data about the new 10-year dividend futures—which are introduced after the third Friday of December each year—are dubious until trading starts properly in January. The December prices of the 10-year dividend futures are often set exactly equal to the prices of the 9-year futures. We therefore disregard the prices of the 10-year futures in any December. The left vertical dashed line in Figure 5 indicates the first day (4 May 2009) of 10 futures being traded (rather than just 7 futures before that day). The slope volatility evidently decreases drastically after that day, but is still larger than after January 2011, when the market seems to be more mature. The right vertical dashed line in Figure 5 marks 3 January 2011, where our observation period starts. The horizontal dashed line marks the average slope over the period starting on 3 January 2011,

$$\bar{s}^{[10]} = \frac{1}{3309} \sum_{t=1}^{3309} s_t^{[10]} = -0.0319.$$

We interpret this value as the unconditional (stationary) slope coefficient for the 10-year maturity.

4 Extraction of fundamental stock-price values

In this section, we describe our approach to extracting the fundamental stock-price values from the dividend-futures data set, using the theoretical models from Section 2. To this end, we partition the fundamental value into three components, with the first two components being directly observable from our data set (Section 4.1), while the third is unobservable and needs to be extrapolated (Section 4.2). We base this extrapolation on insights from a long-run risk model (Section 4.2.2).

4.1 Fundamental-value partitioning

In line with Eq. (10), we compute the fundamental stock-price value at date t, P_t^f, as the sum of all discounted dividend-futures prices ($\widetilde{D}_t^{(m)}$) over infinitely many maturities $m^* = 1, 2, \ldots$. Since our data set only provides dividend-futures prices for the maturities $m^* = 1, \ldots 10$ years, we need to extrapolate the (unobservable) prices for $m^* \geq 11$. We consider the following partitioning of the fundamental value,

$$P_t^f = \mathrm{fv}_{1t} + \mathrm{fv}_{2t} + \mathrm{fv}_{3t}, \tag{16}$$

with the components,

(1) fv_{1t}, calculated with dividend-futures prices of the current year (observable),

(2) fv_{2t}, calculated with prices for $m^* = 2, \ldots, 10$ (observable),

(3) fv_{3t}, calculated with extrapolated prices for $m^* \geq 11$ (unobservable).

Our data set enables us to approximate fundamental values P_t^f according to Eq. (16) for the period between 3 January 2011 and 13 December 2023 (3309 daily observations).

In order to compute the observable component fv_{1t}, we consider the discounted value of the dividend future expiring in the current year m, reduced by the share of dividends that has already been paid out up to day t,

$$\mathrm{fv}_{1t} = \widetilde{D}_t^{(m)} \cdot \frac{D_t^{(m)} - d_t}{D_t^{(m)}}. \tag{17}$$

At the beginning of year m, we have $d_t = 0$ so that $\mathrm{fv}_{1t} = \widetilde{D}_t^{(m)}$. As the dividend payments accumulate over the course of the year, $d_t \to D_t^{(m)}$, so that $\mathrm{fv}_{1t} \to 0$ at the end of year m. The second observable component, fv_{2t}, simply equals the sum of the discounted futures prices for maturities of 2 to 10 years,

$$\mathrm{fv}_{2t} = \sum_{k=1}^{9} \widetilde{D}_t^{(m+k)}, \tag{18}$$

where m again denotes the current year.

4.2 Extrapolated component

4.2.1 Basic assumption

To obtain the component fv_{3t}, we need to extrapolate the remaining discounted dividend-futures prices for maturities of 11 years up to infinity. Denoting the expiry year of the longest running dividend future (which is actually observed) by M with associated maturity $M^* = 10$ years, we write

$$\mathrm{fv}_{3t} = \sum_{k=1}^{\infty} \widetilde{D}_t^{(M+k)}. \tag{19}$$

Eq. (13) now allows us to write

$$\ln\left[\widetilde{D}_t^{(M+k)}\right] = \ln\left[\widetilde{D}_t^{(M)}\right] + \sum_{n=1}^{k} s_t^{[M^*+n]}, \tag{20}$$

and we make the basic assumption that the slope of the discounted maturity curves approaches an average long-run value $\bar{s}^{[\infty]}$ exponentially, i.e.

$$s_t^{[M^*+n]} = \left(s_t^{[M^*]} - \bar{s}^{[\infty]}\right) \cdot \exp\left(-\kappa n\right) + \bar{s}^{[\infty]}, \qquad (\kappa \geq 0). \tag{21}$$

In Eq. (21), $\kappa \geq 0$ determines the speed of convergence towards $\bar{s}^{[\infty]}$, and we have the limiting cases $s_t^{[M^*+n]} = s_t^{[M^*]}$ for $n = 0$, and $s_t^{[M^*+n]} = \bar{s}^{[\infty]}$ for $n \to \infty$.

Using Eqs. (20) and (21), we can now express the third component fv_{3t} in Eq. (19) as follows:

$$\begin{aligned}
\text{fv}_{3t} &= \sum_{k=1}^{\infty} \widetilde{D}_t^{(M+k)} = \sum_{k=1}^{\infty} \widetilde{D}_t^{(M)} \cdot \exp\left(\sum_{n=1}^{k} s_t^{[M^*+n]}\right) \\
&= \widetilde{D}_t^{(M)} \sum_{k=1}^{\infty} \exp\left(\sum_{n=1}^{k} \left[\left(s_t^{[M^*]} - \bar{s}^{[\infty]}\right) \cdot \exp\left(-\kappa n\right) + \bar{s}^{[\infty]}\right]\right) \\
&= \widetilde{D}_t^{(M)} \sum_{k=1}^{\infty} \exp\left(k\bar{s}^{[\infty]} + \left(s_t^{[M^*]} - \bar{s}^{[\infty]}\right) \sum_{n=1}^{k} \exp\left(-\kappa n\right)\right). \qquad (22)
\end{aligned}$$

Since the finite sum inside the exponential expression in Eq. (22) equals $\frac{1-e^{-\kappa k}}{e^{\kappa}-1}$, we have

$$\begin{aligned}
\text{fv}_{3t} &= \widetilde{D}_t^{(M)} \sum_{k=1}^{\infty} \exp\left(k\bar{s}^{[\infty]} + \frac{s_t^{[M^*]} - \bar{s}^{[\infty]}}{e^{\kappa}-1}\left(1 - e^{-\kappa k}\right)\right) \\
&= \widetilde{D}_t^{(M)} \sum_{k=1}^{\infty} \exp\left(k\bar{s}^{[\infty]} + \frac{s_t^{[M^*]} - \bar{s}^{[\infty]}}{e^{\kappa}-1} - e^{-\kappa k}\frac{s_t^{[M^*]} - \bar{s}^{[\infty]}}{e^{\kappa}-1}\right) \\
&= \widetilde{D}_t^{(M)} \exp\left(\frac{s_t^{[M^*]} - \bar{s}^{[\infty]}}{e^{\kappa}-1}\right) \sum_{k=1}^{\infty} \exp\left(k\bar{s}^{[\infty]} - e^{-\kappa k}\frac{s_t^{[M^*]} - \bar{s}^{[\infty]}}{e^{\kappa}-1}\right).
\end{aligned}$$

In our empirical analysis, we truncate the infinite sum on the right side of the last equation at an appropriately selected large value $\bar{k}$, such that the sum of the remaining elements becomes negligible. Thus, we compute the third component as

$$\text{fv}_{3t} = \widetilde{D}_t^{(M)} \exp\left(\frac{s_t^{[M^*]} - \bar{s}^{[\infty]}}{e^{\kappa}-1}\right) \sum_{k=1}^{\bar{k}} \exp\left(k\bar{s}^{[\infty]} - e^{-\kappa k}\frac{s_t^{[M^*]} - \bar{s}^{[\infty]}}{e^{\kappa}-1}\right). \qquad (23)$$

The computation of fv_{3t} in Eq. (23) requires specific choices for the convergence speed κ and the long-run value $\bar{s}^{[\infty]}$. We next address this issue on the basis of a long-run risk model.

4.2.2 Equity yields in a long-run risk model

According to Section 4.2.1, the extraction of the fundamental stock-price value P_t^f is based on an extrapolation of the curve of dividend prices. We can describe this latter curve via the *term structure* of forward equity yields, $e_t^{[n]}$, defined as

$$e_t^{[n]} \equiv \widetilde{D}_t^{[n]} = D_t \cdot \exp\left(-\sum_{k=1}^{n} e_t^{[k]}\right), \qquad (24)$$

where—in line with Eq. (14)—$\widetilde{D}_t^{[n]}$ denotes the price of the dividend claim with maturity in n periods, and $e_t^{[k]}$ is the forward equity yield at time t for the future period from maturity $k-1$ to maturity k.[5]

Table 1 about here

To get an idea of the characteristics of the prices of dividend claims, $\widetilde{D}_t^{[n]}$,and the term structure of forward equity yields, $e_t^{[n]}$, we rely on an equilibrium asset pricing model. Specifically, we use the standard long-run risk model from Bansal and Yaron (2004), in which the expected growth rates of consumption and volatility are stochastic. The dynamics of consumption C, dividends D, and the state variables are given by

$$\Delta \ln C_{t+1} = \mu_c + x_t + \sigma_c \sqrt{V_t}\epsilon_{c,t+1} \tag{25}$$

$$\Delta \ln D_{t+1} = \mu_d + \phi_d x_t + \sigma_{dc} \sqrt{V_t}\epsilon_{c,t+1} + \sigma_{dd} \sqrt{V_t}\epsilon_{d,t+1} \tag{26}$$

$$x_{t+1} = \rho_x x_t + \sigma_x \sqrt{V_t}\epsilon_{x,t+1} \tag{27}$$

$$V_{t+1} = (1-\rho_v)\bar{V} + \rho_v V_t + \sigma_v \epsilon_{v,t+1} \tag{28}$$

where x denotes expected consumption growth and V is the local variance. The innovations $\epsilon_c, \epsilon_d, \epsilon_x, \epsilon_v$ are independent and standard normally distributed. Table 1 contains our parametrization of the model, which is from Bansal et al. (2016). Appendix A presents the formulas for the standard asset pricing moments like the price-dividend ratio, the risk-free rate and the equity risk premium, as well as for the prices of dividend claims and the corresponding term structure of forward equity yields.

For the base parameter set, the equity risk premium is 6.24%, and the risk-free rate 1.6%. The dividend claims for the first 10 years account for around 34% of the price of the fundamental value of the stock. The forward equity yield converges to some long-run level around 7.5% , which is independent of the current values of the state variables.

The convergence of the forward equity yield to some long-run limit follows from the pricing formulas for the dividend claim. The limiting forward equity yield (given in Eq. (A.31) in the Appendix) is independent of the current values of the state variables x and V. For a better economic intuition, note that the forward equity yield for time T follows from the expected behavior of consumption and dividends at T, which in turn is driven by the state variables at time T. Since the distribution of these state variables converges to their stationary distribution when T goes to infinity, their behavior no longer depends on the current levels of x and V. This implies that the limiting forward equity yield also no longer depends on the current levels, and becomes constant.

Figure 6 about here

[5]Recall from Eq. (15) that the forward equity yield is equal to the negative slope of the log dividend price curve, $e_t^{[n]} = -s_t^{[n]}$.

As established in Section 4.2.1 in Eqs. (19) – (23), we endeavor to approximate the forward equity curve by means of an exponential function and the appropriate choice of the two parameters $\bar{e} = -\bar{s}^{[\infty]}$ (the long-term level) and κ (the speed of convergence). Figure 6 shows the combinations $(\bar{e}, \kappa)$ for a variety of parameter sets of the long-run risk model described above. The basic parameters used in Figure 6 are given by the benchmark parameters from Table 1. To generate the scatterplot in Figure 6, we then vary (i) the mean-reversion speeds ρ_x, ρ_v, and (ii) the volatilities σ_x, σ_v of the state variables, each by plus-minus two standard errors. Blue (yellow) points in the scatterplot correspond to parameter combinations $(\bar{e}, \kappa)$ that are close to (far away from) the benchmark case. The limiting level $\bar{e}$ of the forward equity yield curve varies between 0.025 (=2.5%) and 0.15 (=15%), the speed of convergence κ between 0.023 and 0.035.

4.3 Aggregated fundamental values

In accordance with the parameter scales of the theoretical long-run risk model, we now choose appropriate values for κ and $\bar{e} = -s^{[\infty]}$ in order to extrapolate the third component of the fundamental value, fv_{3t}, via Eq. (23) with the dividend-futures data. For this purpose, we extrapolated the third component fv_{3t} with $(\kappa, \bar{e})$ values from a dense grid over $\kappa \in [0.023, 0.035]$ and $\bar{e} \in [0.025, 0.15]$. For many of the $(\kappa, \bar{e})$-combinations on the grid, the resulting aggregate fundamental $P_t^f = \text{fv}_{1t} + \text{fv}_{2t} + \text{fv}_{3t}$ exceeds the EuroStoxx index on some trading days, implying negative bubble values B_t on those days. Since negative (rational) bubble values are ruled out by the Diba and Grossman (1988b) conditions (Section 2.1), we focused on $(\kappa, \bar{e})$-combinations that entail positive bubble values throughout the sampling period. The red dots in Figure 6 delineate the border between $(\kappa, \bar{e})$-combinations resulting in (at least one) negative bubble values (to the left of the border) and combinations that yield exclusively positive bubble values (to the right). Among the admissible combinations, we selected the specific values $\kappa = 0.0295$ and $\bar{e} = 0.11$, which are represented by the red cross in Figure 6. Since this combination is inside the light blue area, we interpret this parameter choice as being consistent with the long-run risk model of Bansal and Yaron (2004), Bansal et al. (2016).

Figure 7 about here

Figure 7 shows the three fundamental components $\text{fv}_{1t}, \text{fv}_{2t}, \text{fv}_{3t}$ over time. Panel (a) reveals that the component fv_{1t} (dividends accruing in the current year) is almost negligible. The component fv_{2t} (dividends accruing up to 10 years into the future) in Panel (b) is significant, but still only accounts for a limited part of the aggregated fundamental values P_t^f. Obviously, it is the extrapolated component fv_{3t} in Panel (c) that makes up the largest portion of P_t^f.

5 Bubble component

Figure 8 about here

5.1 Explorative data analysis

Figure 8 shows (1) the EuroStoxx50 (P_t, left axis), (2) the aggregated fundamental (P_t^f, left axis), (3) the bubble component ($B_t = P_t - P_t^f$, left axis), and (4) the share of the bubble component in the index, calculated as B_t/P_t (right axis), in a single line graph. In 'normal' phases of the market, the bubble share in the index fluctuates between 13% (0.1-quantile: 0.136) and 33% (0.9-quantile: 0.321) around a mean value of 22% (arithmetic mean: 0.218, median: 0.214). Figure 8 shows three important events in which the bubble share—and also the nominal bubble values themselves—decline towards zero. (1) The bubble share begins to decline shortly after the annexation of Crimea (March 18, 2014) and reaches its historic low of 0.003 (= 0.3%) on January 12, 2015, shortly before the signing of the Minsk-II agreement on February 12, 2015. (2) On March 18, 2020, seven days after the World Health Organization (WHO) classified COVID-19 as a pandemic, the bubble share fell to 0.009 (= 0.9%). (3) Shortly after the start of the war in Ukraine on February 24, 2022, the bubble share fell to 0.14 (= 14%) on March 7, 2022 due to the perceived increase in geopolitical risks.

Figure 9 about here

Table 2 about here

Figure 9 shows the histograms of the daily bubble and fundamental returns. Both return series can be well fitted by t-distributions with 2.2 (bubble) and 3.5 (fundamental) degrees of freedom; see Table 2. The bubble returns are quite volatile with an estimated annualized standard deviation of 1.905. The estimated annualized volatility for the fundamental returns is 0.307, which is much lower than the volatility of the bubble returns, but still higher than the volatility of the EuroStoxx index returns (0.201). This could explain the negative correlation of −0.418 between the bubble and the fundamental returns shown in the lower block of Table 2. The first-order autocorrelation coefficients of the bubble and the fundamental returns are negative (−0.314, −0.185), while the autocorrelation of the index returns is close to zero (−0.001).

Table 3 about here

Table 3 shows the results of some selected tests for explosiveness and variance-ratio

applied to the EuroStoxx50, the fundamental and bubble series and the corresponding log values. The RADF and SADF tests for explosiveness, adopted from Phillips et al. (2011) and Phillips et al. (2015), are based on (appropriately defined) sequences of t-(ADF-)statistics of the parameter θ estimated from the specification

$$y_t = c + \theta \cdot y_{t-1} + \sum_{i=1}^{k} \phi_i \cdot \Delta y_{t-i} + \epsilon_t, \tag{29}$$

where y_t represents the series P_t, P_t^f, B_t (and their logs), k is a given lag order, Δ is the difference operator, and $\epsilon_t \overset{\text{i.i.d.}}{\sim} (0, \sigma^2)$. The general aim is to test the unit-root null hypothesis $H_0 : \theta = 1$ (time series is not explosive, indicated by 'No' in Table 3) versus the right-tailed alternative $H_1 : \theta > 1$ (time series is explosive, indicated by 'Yes' in Table 3).

While the RADF test is based on the maximum ADF statistic from a rolling window, the SADF test statistic is the supremal (maximum) ADF statistic from an (appropriately defined) expanding window. The critical values of both tests were determined by bootstrap simulations for which we used the routines implemented in the EViews 14 software. In particular, we (1) performed all tests by setting the lag order k in Eq. (29) to 4, and (2) obtained the 'Yes/No' explosiveness-decisions by testing at the 5% significance level. In Table 3, the realizations of the RADF/SADF test statistics are given in round brackets below the 'Yes/No' decisions, where *, **, *** denote significance at the 10, 5, and 1% levels, respectively.

The specific results in terms of explosiveness in Table 3 appear to be somewhat ambiguous. According to the RADF tests, neither the EuroStoxx50 nor the fundamental series (nor their logs) display significant explosive behavior. In contrast, the bubble series B_t and $\log(B_t)$ display explosive behavior at the 1% level. However, when using the SADF tests, explosiveness in the bubble series is no longer statistically detectable.

The last two columns of Table 3 show the results of some variance ratio (VR) tests in order to answer the question of whether the data in the series follow a martingale and/or a random walk. Specifcally, we use the routines in Eviews 14, which are built upon the test variants from Lo and MacKinlay (1988, 1989). The null hypothesis of these VR tests is that the series is a martingale/random walk. Technically, we first compute individual VR tests for the respective periods 2, 5, 10, 30 (with the test statistics z_2, z_5, z_{10}, z_{30}) and then conduct the multiple VR test using the joint test statistic $\max\{|z_2|, |z_5|, |z_{10}|, |z_{30}|\}$ proposed by Chow and Denning (1993). In Table 3, we obtain the VR 'Yes/No' decisions by conducting the multiple Chow-Denning test at the 5% level. Interestingly, the EuroStoxx50 data (and its log) are consistent with a martingale and/or random-walk, while the fundamental series (and its log) differs significantly from both process types. Similarly, the bubble series (B_t) deviates significantly from a martingale/random walk, while the log bubble may be viewed as consistent with a martingale (when tested at the 5% level).

5.2 Estimation of bubble specification

We now turn to estimating of the (flexibilized) Rotermann and Wilfling (2018) bubble specification from Eq. (11). The logarithmic bubble $b_t = \log(B_t)$ is distributed as the following mixture of two normal distributions,

$$b_{t+1} = \begin{cases} \mathbb{N}(b_t + \ln[\alpha/(\psi_t \pi)] - \sigma^2/2, \sigma^2) & , \text{ with probability } \pi \\ \mathbb{N}(b_t + \ln[(1-\alpha)/(\psi_t(1-\pi))] - \sigma^2/2, \sigma^2) & , \text{ with probability } 1-\pi \end{cases}, \tag{30}$$

where (i) $\psi_t = (1 + r_t)^{-1}$ with r_t denoting the one-period (risk-free) interest rate, and (ii) the parameters (to be estimated) α, π, σ, which should be subject to the rationality conditions $0 < \alpha < 1, (\alpha/\pi) > 1$ and $1 - \alpha < \psi_t(1 - \pi)$ for all t. The log-likelihood function is given by

$$\ln\left[\mathcal{L}(\alpha, \pi, \sigma)\right] = \sum_{t=2}^{T} \ln\left[\pi \cdot f_1(b_t|b_{t-1}) + (1-\pi) \cdot f_2(b_t|b_{t-1})\right], \tag{31}$$

with $f_1(\cdot|\cdot)$ and $f_2(\cdot|\cdot)$ denoting the density functions of the two Gaussian mixture components.

Table 4 about here

In a first step, we maximize the log-likelihood (31) with respect to α, π, σ, using a numerical algorithm that considers inequality constraints and bounds on the parameters (module FMINCON from the R-package PRACMA). The maximum log-likelihood value is 4370.768. Not surprisingly (given the constraints), the lower block of Table 4 confirms that (i) all rationality restrictions are fulfilled at all points in time, and (ii) the optimum is in the interior of the parameter space. In a second step, we examine whether the constrained estimates differ significantly from their unconstrained counterparts. To this end, we re-estimated the bubble specification without imposing the rationality conditions in the bottom block of Table 4 (keeping the conditions $\alpha, \pi \in (0, 1), \sigma > 0$). These 'unrestricted' estimates are found to be identical to the restricted estimates in Table 4 (with the same maximum log-likelihood value 4370.768). Obviously, the rationality conditions from above are not binding, i.e. the estimated bubble process satisfies the rationality conditions without enforcing them.

6 Conclusion

In this article, we extract the bubble and fundamental components of the EuroStoxx50 index for the period from January 2011 to December 2023 (3309 trading days). Our econometric method combines a theoretical bubble specification and a novel data set of dividend futures prices. Our data-driven methodology refrains from estimating highly parameterized equations and thus avoids estimation errors, but relies on extrapolating the forward equity yield

curve. The impact of our extrapolation on the extracted bubble values is an interesting question that we leave for future research.

The (statistical) properties of the extracted EuroStoxx50 bubble are in close agreement with the relevant economic/financial intuition. During the observation period, the bubble share in the index fluctuated around 22% and reacted sharply to significant external events, such as the two military attacks on Ukraine (annexation of Crimea in 2014, start of war in 2022) and the outbreak of COVID-19 (in spring 2020). Obviously, market participants responded to the increasing perceived geopolitical risks and/or the uncertain economic outlook by valuing the EuroStoxx50 index primarily on the basis of fundamentals, and largely pushing speculative motives into the background. Apart from such *ex-post* evidence, we believe that our bubble extraction methodology can provide additional useful information to economic agents. With the available dividend-futures data set, the method can be adapted for real-time monitoring of fundamental and bubble values with little computational effort.

In Section 5.1 (Table 3), we test the EuroStoxx and its fundamental and bubble components for explosiveness. The RADF and SADF tests and their many variants have become important and widely used tools for detecting explosive bubble-like behavior in financial time series. Several authors have mentioned that the specific test result (explosiveness 'Yes/No') often crucially depends '[. . .] on the way the [testing] procedures are implemented and on the maintained assumptions about the underlying data-generating mechanism' (Caravello et al., 2023). In view of this, a future research direction could be to check a large set of bubble trajectories extracted with our methodology for specific statistical properties. Heteroscedasticity patterns (conditional and unconditional) should play a major role in this context, as time-varying volatility has been a key argument for the introduction of recent test variants (e.g. Harvey et al., 2020). The detected statistical properties could assist econometricians in selecting a suitable test variant from the many available.

Appendix

A Long-run risk model

A.1 Model setup

We consider a long-run risk model, following Bansal and Yaron (2004), with stochastic expected growth and stochastic volatility. The dynamics of aggregate consumption are

$$\Delta \ln C_{t+1} = \mu_c + x_t + \sigma_c \sqrt{V_t}\epsilon_{c,t+1}, \tag{A.1}$$

with expected consumption growth rate x and the local variance V given by

$$x_{t+1} = \rho_x x_t + \sigma_x \sqrt{V_t}\epsilon_{x,t+1}, \tag{A.2}$$

$$V_{t+1} = (1-\rho_v)\bar{V} + \rho_v V_t + \sigma_v \epsilon_{v,t+1}, \tag{A.3}$$

where ϵ_c, ϵ_x, and ϵ_v are independent standard normally distributed random variables.

The representative investor has Epstein-Zin preferences with relative risk aversion γ and intertemporal elasticity of substitution ψ. We assume $\gamma, \psi > 1$, which implies a preference for early resolution of uncertainty. We set $\theta = \frac{1-\gamma}{1-\frac{1}{\psi}}$.

The log pricing kernel m is given by

$$m_{t+1} = \theta \ln \delta - \frac{\theta}{\psi} \Delta \ln C_{t+1} - (1-\theta) \ln R_{c,t+1}, \tag{A.4}$$

where $R_{c,t+1}$ is the return on the consumption claim. For this return, we rely on the Campbell-Shiller approximation

$$\ln R_{c,t+1} = \kappa_{c,0} + \kappa_{c,1} w_{t+1} - w_t + \Delta \ln C_{t+1}, \tag{A.5}$$

where w is the log price-consumption ratio. The linearization coefficients $\kappa_{c,0}$ and $\kappa_{c,1}$ are given by

$$\kappa_{c,0} = -\kappa_{c,1} \ln \kappa_{c,1} - (1-\kappa_{c,1}) \ln(1-\kappa_{c,1}), \tag{A.6}$$

$$\kappa_{c,1} = \frac{e^{E[w]}}{1+e^{E[w]}}. \tag{A.7}$$

For w, we rely on the affine guess $w_t = A_{c,0} + A_{c,x} x_t + A_{c,v} V_t$.

Next, we present the results which we need for analyzing dividend claims. A more detailed derivation can be found in the Online Appendix.

A.2 Consumption claim

The consumption claim has to satisfy the Euler equation,

$$E\left[e^{m_{t+1} + \ln R_{c,t+1}}\right] = 1. \tag{A.8}$$

Plugging the Campbell-Shiller approximation (A.5) for the return and the functional form (A.4) of the stochastic discount factor into the Euler equation (A.8) allows us to solve for the coefficient functions of the wealth-consumption ratio:

$$A_{c,0} = \frac{\ln \delta + \left(1-\frac{1}{\psi}\right)\mu_c + \kappa_{c,0} + \kappa_{c,1} A_{c,V} (1-\rho_v) \bar{V} + 0.5\theta \kappa_{c,1}^2 A_{c,V}^2 \sigma_v^2}{1-\kappa_{c,1}}, \tag{A.9}$$

$$A_{c,x} = \frac{1-\frac{1}{\psi}}{1-\kappa_{c,1}\rho_x}, \tag{A.10}$$

$$A_{c,V} = \frac{0.5(1-\gamma)\left(1-\frac{1}{\psi}\right)\sigma_c^2 + 0.5\theta \kappa_{c,1}^2 A_{c,x}^2 \sigma_x^2}{1-\kappa_{c,1}\rho_v}. \tag{A.11}$$

A.3 Stochastic discount factor

The stochastic discount factor is given in (A.4). Plugging in the Campbell-Shiller equation (A.5) for the return on the consumption claim and the affine functional form of the wealth-consumption ratio yields

$$m_{t+1} = m_0 + m_x x_t + m_v V_t - \lambda_c \sqrt{V_t}\epsilon_{c,t+1} - \lambda_x \sqrt{V_t}\epsilon_{x,t+1} - \lambda_v \epsilon_{v,t+1}, \tag{A.12}$$

where

$$\begin{aligned} m_0 &= \theta \ln \delta - \gamma\mu_C + (\theta-1)\kappa_{c,0} - (\theta-1)(1-\kappa_{c,1})A_{c,0} + (\theta-1)\kappa_{c,1}A_{c,V}(1-\rho_v)\bar{V}, \\ m_x &= (1-\theta)(1-\kappa_{c,1}\rho_x)A_{c,x} - \gamma, \\ m_v &= (1-\theta)(1-\kappa_{c,1}\rho_v)A_{c,V}. \end{aligned} \tag{A.13}$$

The market prices of risk are

$$\begin{aligned} \lambda_c &= \gamma\sigma_c, \\ \lambda_x &= (1-\theta)\kappa_{c,1}A_{c,x}\sigma_x, \\ \lambda_v &= (1-\theta)\kappa_{c,1}A_{c,V}\sigma_v. \end{aligned}$$

A.4 Fundamental price of the stock

The dynamics of the dividends are given by

$$\Delta \ln D_{t+1} = \mu_d + \phi_d x_t + \sigma_{dc}\sqrt{V_t}\epsilon_{c,t+1} + \sigma_{dd}\sqrt{V_t}\epsilon_{d,t+1}. \tag{A.14}$$

The stock has to satisfy the Euler equation

$$E\left[e^{m_{t+1}+\ln R_{d,t+1}}\right] = 1. \tag{A.15}$$

Plugging the Campbell-Shiller approximation for the return (analogous to (A.5)), a linear guess for the log price-dividend ratio $w_d = A_{d,0} + A_{d,x}x_t + A_{d,v}V_t$, and the dynamics of the state variables into the Euler equation (A.15) yields

$$A_{d,0} = \frac{m_0 + \kappa_{d,0} + \kappa_{d,1}A_{d,V}(1-\rho_v)\bar{V} + \mu_d + 0.5\left(\kappa_{d,1}A_{d,v}\sigma_v - \lambda_v\right)^2}{1-\kappa_{d,1}}, \tag{A.16}$$

$$A_{d,x} = \frac{m_x + \phi_d}{1-\kappa_{d,1}\rho_x}, \tag{A.17}$$

$$A_{d,V} = \frac{m_v + 0.5\left(\sigma_{dc} - \lambda_c\right)^2 + 0.5\left(\kappa_{d,1}A_{d,x}\sigma_x - \lambda_x\right)^2 + 0.5\sigma_{dd}^2}{1-\kappa_{d,1}\rho_v}. \tag{A.18}$$

A.5 Dividend claims

The price of the dividend claims, i.e. the claims to only one future dividend, follows recursively. For the first dividend claim, we obtain

$$\widetilde{D}_t^{[1]} = D_t \mathbb{E}_t\left[e^{m_{t+1}+\Delta \ln D_{t+1}}\right] = D_t e^{ds_0^{[1]}+ds_x^{[1]}x_t+ds_v^{[1]}V_t}, \tag{A.19}$$

where

$$ds_0^{[1]} = m_0 + \mu_d + 0.5(-\lambda_v)^2, \tag{A.20}$$
$$ds_x^{[1]} = m_x + \phi_d, \tag{A.21}$$
$$ds_v^{[1]} = m_v + 0.5(\sigma_{dc} - \lambda_c)^2 + 0.5(-\lambda_x)^2 + 0.5(\sigma_{dd})^2. \tag{A.22}$$

For the $(n+1)$st dividend claim, we obtain

$$\widetilde{D}_t^{[n+1]} = \mathbb{E}_t\left[e^{m_{t+1}}\widetilde{D}_{t+1}^{[n]}\right] = D_t e^{ds_0^{[n+1]}+ds_x^{[n+1]}x_t+ds_v^{[n+1]}V_t}, \tag{A.23}$$

where

$$ds_0^{[n+1]} = m_0 + \mu_d + ds_0^{[n]} + ds_v^{[n]}(1-\rho_v)\bar{V} + 0.5(ds_v^{[n]}\sigma_v - \lambda_v)^2, \tag{A.24}$$
$$ds_x^{[n+1]} = m_x + \phi_d + ds_x^{[n]}\rho_x, \tag{A.25}$$
$$ds_v^{[n+1]} = m_v + ds_v^{[n]}\rho_v + 0.5(\sigma_{dc} - \lambda_c)^2 + 0.5(ds_x^{[n]}\sigma_x - \lambda_x)^2 + 0.5(\sigma_{dd})^2. \tag{A.26}$$

The forward equity yields are

$$e_t^{[n+1]} = ds_0^{[n+1]} - ds_0^{[n]} + \left(ds_x^{[n+1]} - ds_x^{[n]}\right)x_t + \left(ds_v^{[n+1]} - ds_v^{[n]}\right)V_t. \tag{A.27}$$

The limiting values for $n \to \infty$ are

$$\lim_{n\to\infty} ds_0^{[n+1]} - ds_0^n = m_0 + \mu_d + ds_v^{[\infty]}(1-\rho_v)\bar{V} + 0.5(ds_v^{[\infty]}\sigma_v - \lambda_v)^2, \tag{A.28}$$
$$\lim_{n\to\infty} ds_x^{[n]} = \frac{m_x + \phi_d}{1-\rho_x}, \tag{A.29}$$
$$\lim_{n\to\infty} ds_v^{[n]} = \frac{m_v + 0.5(\sigma_d - \lambda_c)^2 + 0.5(ds_x^{[\infty]}\sigma_x - \lambda_x)^2 + 0.5(\sigma_{dd})^2}{1-\rho_v}. \tag{A.30}$$

The limit of the forward equity yield for $n \to \infty$ is thus given by

$$e_t^{\infty} = \lim_{n\to\infty} ds_0^{[n+1]} - ds_0^{[n]}, \tag{A.31}$$

and no longer depends on the state variables.

References

Abreu, D. and M. K. Brunnermeier (2003). Bubbles and crashes. Econometrica 71(1), 173–204.

Al-Anaswah, N. and B. Wilfling (2011). Identification of speculative bubbles using state-space models with Markov-switching. Journal of Banking and Finance 35(5), 1073–1086.

Allen, F. and D. Gale (2000). Bubbles and crises. Economic Journal 110(460), 236–255.

Allen, F. and G. Gorton (1993). Churning bubbles. Review of Economic Studies 60(4), 813–836.

Balke, N. S. and M. E. Wohar (2009). Market fundamentals versus rational bubbles in stock prices: A Bayesian perspective. Journal of Applied Econometrics 24(1), 35–75.

Bansal, R., D. Kiku, and A. Yaron (2016). Risks for the long run: Estimation with time aggregation. Journal of Monetary Economics 82(1), 52–69.

Bansal, R. and A. Yaron (2004). Risks for the long run: A potential resolution of asset pricing puzzles. Journal of Finance 59(4), 1481–1509.

Barberis, N., R. Greenwood, L. Jin, and A. Shleifer (2018). Extrapolation and bubbles. Journal of Financial Economics 129, 203–227.

Blasques, F., S. Koopman, G. Mingoli, and S. Telg (2024). A novel test for the presence of local explosive dynamics. Tinbergen Institute Discussion Paper TI 2024-036/111, Tinbergen Institut, Amsterdam and Rotterdam.

Bordalo, P., S. Gennaioli, Y. Kwon, and A. Shleifer (2021). Diagnostic bubbles. Journal of Financial Economics 141, 1060–1077.

Braggion, F., R. Frehen, and E. Jerphanion (2023). Credit provision and stock trading: Evidence from the south sea bubble. Journal of Financial and Quantitative Analysis, 1–31. doi:10.1017/S0022109023001163.

Campbell, J. Y., A. W. Lo, and M. A. Craig (1997). The Econometrics of Financial Markets. Princeton University Press: Princeton.

Campbell, J. Y. and R. J. Shiller (1988a). The dividend-price ratio and expectations of future dividends and discount factors. Review of Financial Studies 1(3), 195–228.

Campbell, J. Y. and R. J. Shiller (1988b). Stock prices, earnings, and expected dividends. Journal of Finance 43(3), 661–676.

Caravello, T. E., Z. Psaradakis, and M. Sola (2023). Rational bubbles: Too many to be true? Journal of Economic Dynamics & Control 151(Article no. 104666), 1–27.

Chan, J. C. C. and C. Santi (2021). Speculative bubbles in present-value models: A Bayesian Markov-switching state space approach. Journal of Economic Dynamics & Control 127, Article 104101.

Chow, K. V. and K. C. Denning (1993). A simple multiple variance ratio test. Journal of Econometrics 58(3), 385–401.

Cochrane, J. H. (2005). Asset Pricing – Revised Edition. Princeton University Press.

Cochrane, J. H. (2011). Presidential address: Discount rates. Journal of Finance 66(4), 1047–1108.

Cuthbertson, K. and D. Nitzsche (2004). Quantitative Financial Economics: Stocks, Bonds and Foreign Exchange. Wiley: New York.

Diba, B. T. and H. I. Grossman (1988a). Explosive rational bubbles in stock prices? American Economic Review 78(3), 520–530.

Diba, B. T. and H. I. Grossman (1988b). The theory of rational bubbles in stock prices. Economic Journal 98(392), 746–754.

Enders, Z. and H. Hakenes (2021). Market depth, leverage, and speculative bubbles. Journal of the European Economic Association 19(5), 2577–2621.

Engsted, T., T. Pedersen, and C. Tanggaard (2012). The log-linear return approximation, bubbles, and predictability. Journal of Financial and Quantitative Analysis 47(3), 643–665.

Evans, G. W. (1991). Pitfalls in testing for explosive bubbles in asset prices. American Economic Review 81(4), 922–930.

Fukuta, Y. (1998). A simple discrete-time approximation of continuous-time bubbles. Journal of Economic Dynamics & Control 22(6), 937–954.

Hafner, C. M. (2018). Testing for bubbles in cryptocurrencies with time-varying volatility. Journal of Financial Econometrics 18(2), 233–249.

Hall, S. G., Z. Psaradakis, and M. Sola (1999). Detecting periodically collapsing bubbles: A Markov-switching unit root test. Journal of Applied Econometrics 14(2), 143–154.

Harvey, D. I., S. J. Leybourne, and Y. Zu (2020). Sign-based unit root tests for explosive financial bubbles in the presence of deterministically time-varying volatility. Econometric Theory 36(1), 122–169.

Homm, U. and J. Breitung (2012). Testing for speculative bubbles in stock markets: A comparison of alternative methods. Journal of Financial Econometrics 10(1), 198–231.

Kurozumi, E. (2020). Asymptotic properties of bubble monitoring tests. Econometric Reviews 39(5), 510–538.

Lammerding, M., P. Stephan, M. Trede, and B. Wilfling (2013). Speculative bubbles in recent oil-price dynamics: Evidence from a Bayesian Markov-switching state-space approach. Energy Economics 36(1), 491–502.

Lo, A. W. and A. C. MacKinlay (1988). Stock market do not follow random walks: Evidence from a simple specification test. Review of Financial Studies 1(1), 41–66.

Lo, A. W. and A. C. MacKinlay (1989). The size and power of the variance ratio test in finite sample: A Monte Carlo investigation. Journal of Econometrics 40(2), 203–238.

Lui, Y. L., P. C. B. Phillips, and J. Yu (2024). Robust testing for explosive behavior with strongly dependent errors. Journal of Econometrics 238(2), Article 105626.

Monschang, V. and B. Wilfling (2021). Sup-ADF-style bubble-detection methods under test. Empirical Economics 61(1), 145–172.

Morita, R., Z. Psaradakis, M. Sola, and P. Yunis (2023). On testing for bubbles during hyperinflations. Studies in Nonlinear Dynamics & Econometrics, doi: https://doi.org/10.1515/snde–2022–0014.

Phillips, P. C. B., S.-P. Shi, and J. Yu (2015). Testing for multiple bubbles: Historical episodes of exuberance and collapse in the S&P 500. International Economic Review 56(4), 1043–1078.

Phillips, P. C. B., Y. Wu, and J. Yu (2011). Explosive bahavior in the 1990s NASDAQ: When did exuberance escalate asset values? International Economic Review 52(1), 201–226.

Rotermann, B. and B. Wilfling (2014). Peridically collapsing evans bubbles and stock-price volatility. Economics Letters 123(3), 383–386.

Rotermann, B. and B. Wilfling (2018). A new stock-price bubble with stochastically deflating trajectories. Applied Economics Letters 25(15), 1091–1096.

Shi, S. and Y. Song (2016). Identifying speculative bubbles using an infinite hidden Markov model. Journal of Financial Econometrics 14(1), 159–184.

Tirole, J. (1982). On the possibility of speculation under rational expectations. Econometrica 50(1), 1163–1181.

Tirole, J. (1985). Asset bubbles and overlapping generations. Econometrica 53(6), 1499–1528.

van Binsbergen, J., W. Hueskes, R. Koijen, and E. Vrugt (2013). Equity yields. Journal of Financial Economics 110(3), 503–519.

Wu, Y. (1995). Are there rational bubbles in foreign exchange markets? evidence from an alternative test. Journal of International Money and Finance 14(1), 27–46.

Wu, Y. (1997). Rational bubbles in the stock market: accounting for the us stock-price volatility. Economic Inquiry 35(2), 309–319.

Tables and Figures

Table 1: Parameters of long-run risk model: Benchmark

Parameter	Value	Parameter	Value	Parameter	Value	Standard error
γ	9.67	μ_c	0.0016	ρ_x	0.9762	(0.0035)
ψ	2.18	μ_d	0.0016	σ_x	0.0318	(0.0053)
β	0.9990	ϕ_d	4.51	ρ_v	0.9984	(0.0007)
		σ_{dc}	2.3715	$\bar{V}$	0.0070^2	
		σ_{dd}	4.0	σ_v	2.12e-6	(5.32e-7)

Notes: The parameters are from Bansal et al. (2016). The decision interval is $\Delta_t = 1/11$. For the mean reversion speed and the volatilities of the state variables, we also give the standard errors.

Table 2: Descriptive statistics and correlations

Descriptive statistics (estimates)					
	Bubble returns		Fundamental returns		Index returns
t-distr. dgf	2.200		3.500		
Ann. std. dev.	1.905		0.307		0.201
AR(1) coef.	−0.314		−0.185		−0.001
Correlations of returns (estimates)					
	P_t^f	B_t	P_t	fv_2	fv_3
P_t^f	1.000	−0.418	0.573	0.449	0.945
B_t		1.000	0.223	−0.012	−0.459
P_t			1.000	0.441	0.468
fv_2				1.000	0.197
fv_3					1.000

Notes: $P_t^f, B_t, P_t, \mathrm{fv}_2, \mathrm{fv}_3$ denote the fundamental value, the bubble component, and the index values of the EuroStoxx, respectively. $\mathrm{fv}_2, \mathrm{fv}_3$ are fundamental-value components from Eqs. (18), (23).

Table 3: Explosiveness and Variance Ratio (VR) tests

	Tests for explosiveness		Variance ratio tests	
	RADF	SADF	Martingale	Random walk
Eurostoxx50 (P_t)	No	No	Yes	Yes
	(1.50)	(1.40)	(0.72)	(1.02)
$\log(P_t)$	No	Yes	Yes	Yes
	1.86)	(1.79^{**})	(0.75)	(1.17)
Fundamental (P_t^f)	No	No	No	No
	(1.82)	(0.57)	(7.40^{***})	(11.17^{***})
$\log(P_t^f)$	No	No	No	No
	(2.20)	(0.92)	(6.88^{***})	(10.59^{***})
Bubble (B_t)	Yes	No	No	No
	(3.79^{***})	(−0.55)	(9.36^{***})	(14.36^{***})
$\log(B_t)$	Yes	No	Yes	No
	(6.95^{***})	(0.60)	(1.82)	(18.05^{***})

Notes: P_t, P_t^f, B_t respectively denote the index values of Eurostoxx50, the fundamental and the bubble series.

For the RADF and SADF tests, the null hypothesis is that the series is not explosive. For all tests, Eq. (29) is specified with $k = 4$ lags. Throughout the entire table, the entries in round brackets are the realizations of the corresponding test statistics. *, **, *** denote significance at the 10, 5, and 1% levels. For RADF/SADF the test decision is classified as 'Yes (series is explosive)', if the realized test statistic is significant at the 5% level.

The null hypothesis of the variance ratio tests is that the series is a martingale/random walk. For both VR tests, we show (in round brackets) the multiple Chow and Denning (1993) maximum test statistic, computed from the individual VR tests for the periods 2, 5, 10, 30 (see Section 5.1). We classify the test decision as 'No (series is not a martingale/random walk)' if the multiple Chow-Denning maximum test statistic is significant at the 5% level.

Table 4: Estimation of the Rotermann and Wilfling (2018) bubble

Parameter	Estimate	Standard error
α	0.9994	0.0003
π	0.9986	0.0007
σ	0.0639	0.0008
Max. logl-value: 4370.768		
Rationality conditions:		
α/π	1.0009	
$\frac{1-\alpha}{1-\pi}$	0.3847	
Range ψ_t	(0.99989, 1.00003)	

Notes: $\alpha, \pi, \sigma, \psi_t$ are as in the parametric bubble specification from Eq. (30).

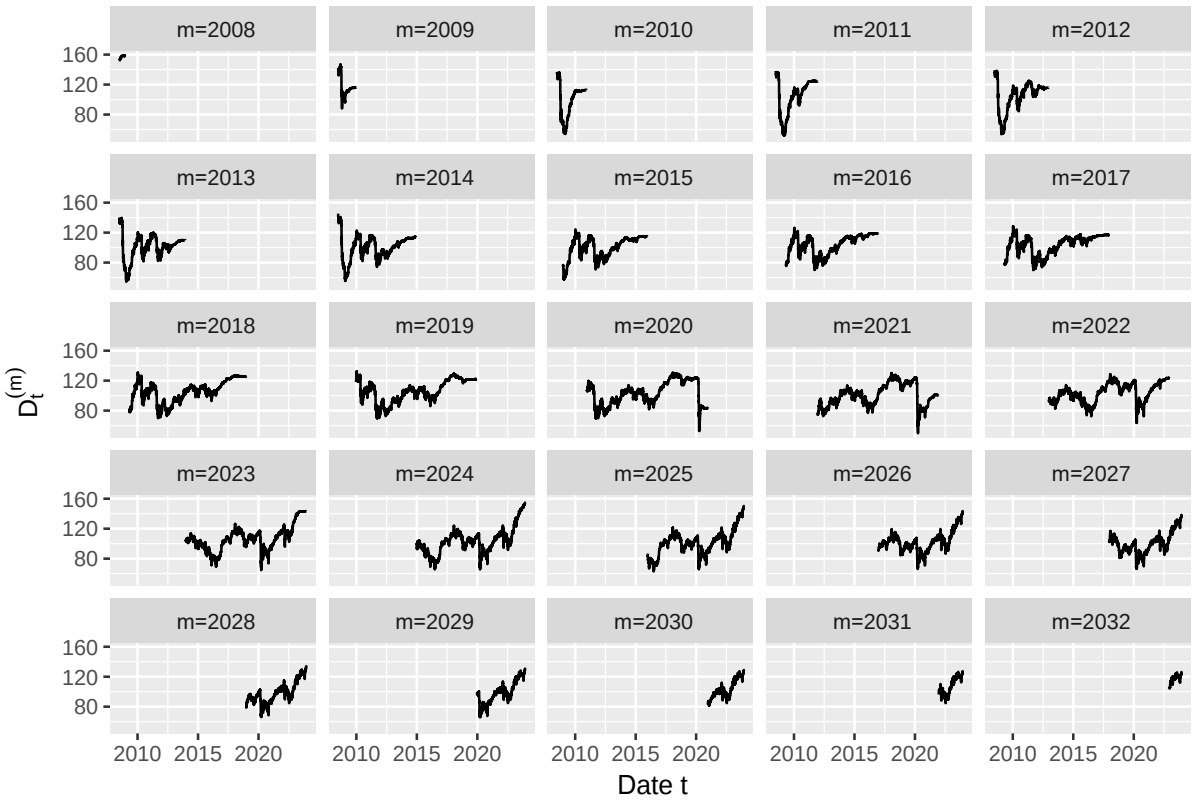

Figure 1: Dividend-futures prices

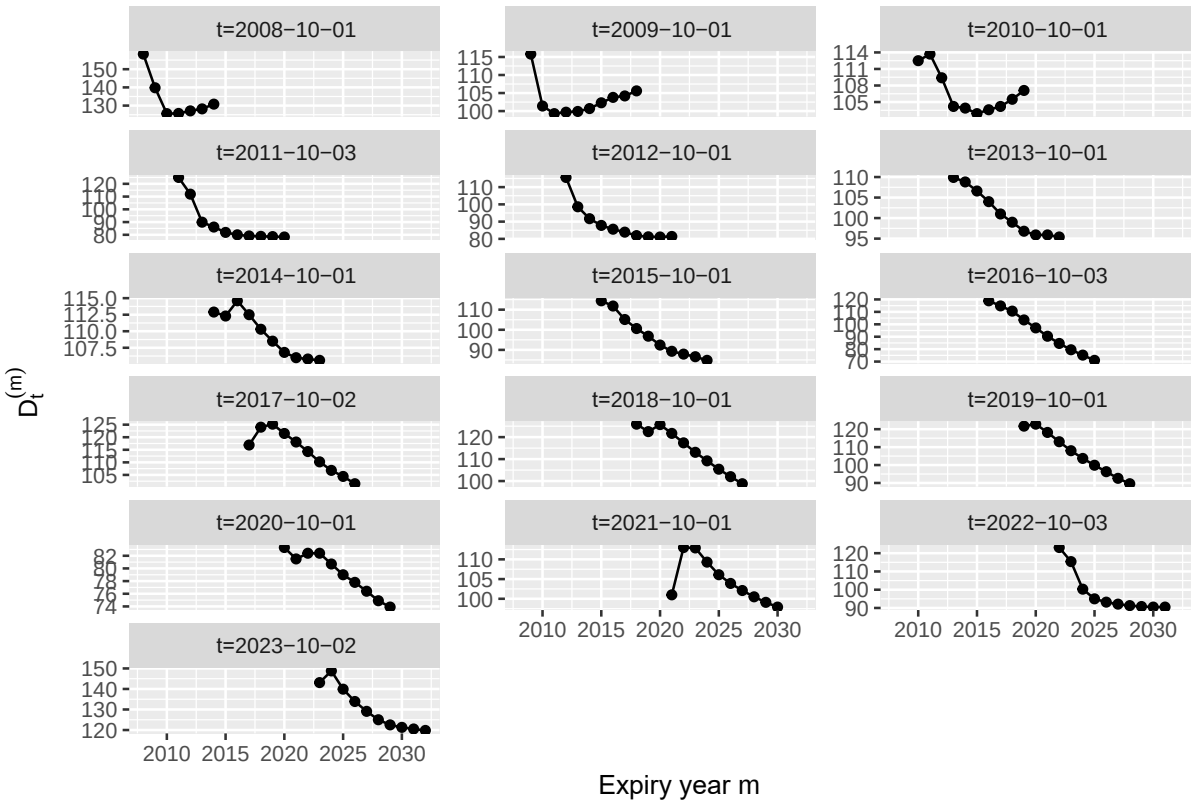

Figure 2: Maturity curves

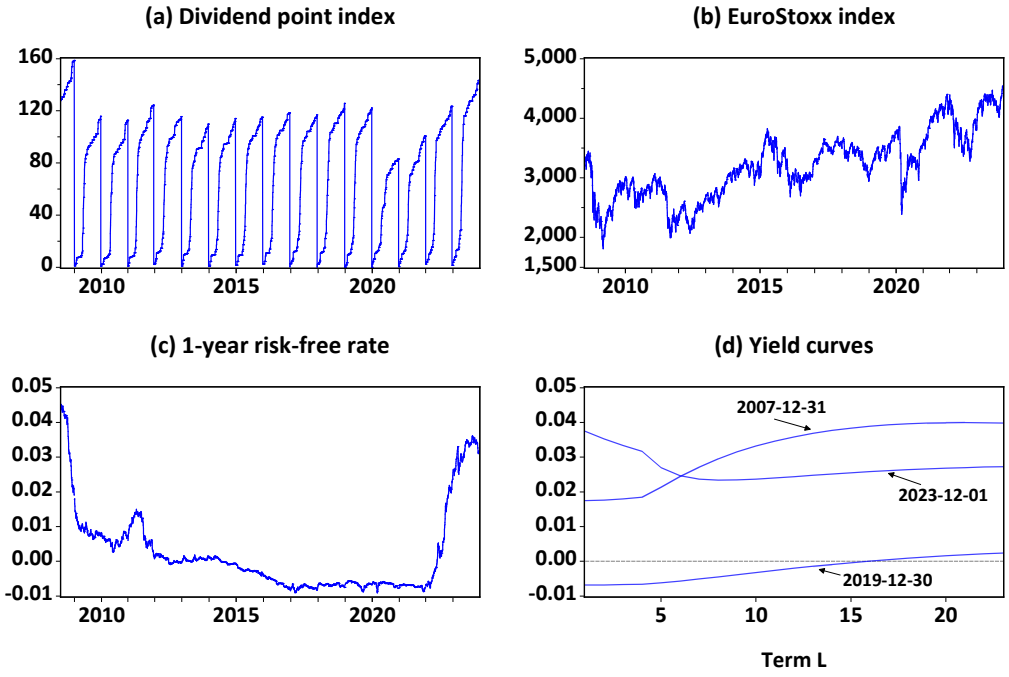

Figure 3: Dividend point index, EuroStoxx index, risk-free rate, yield curves

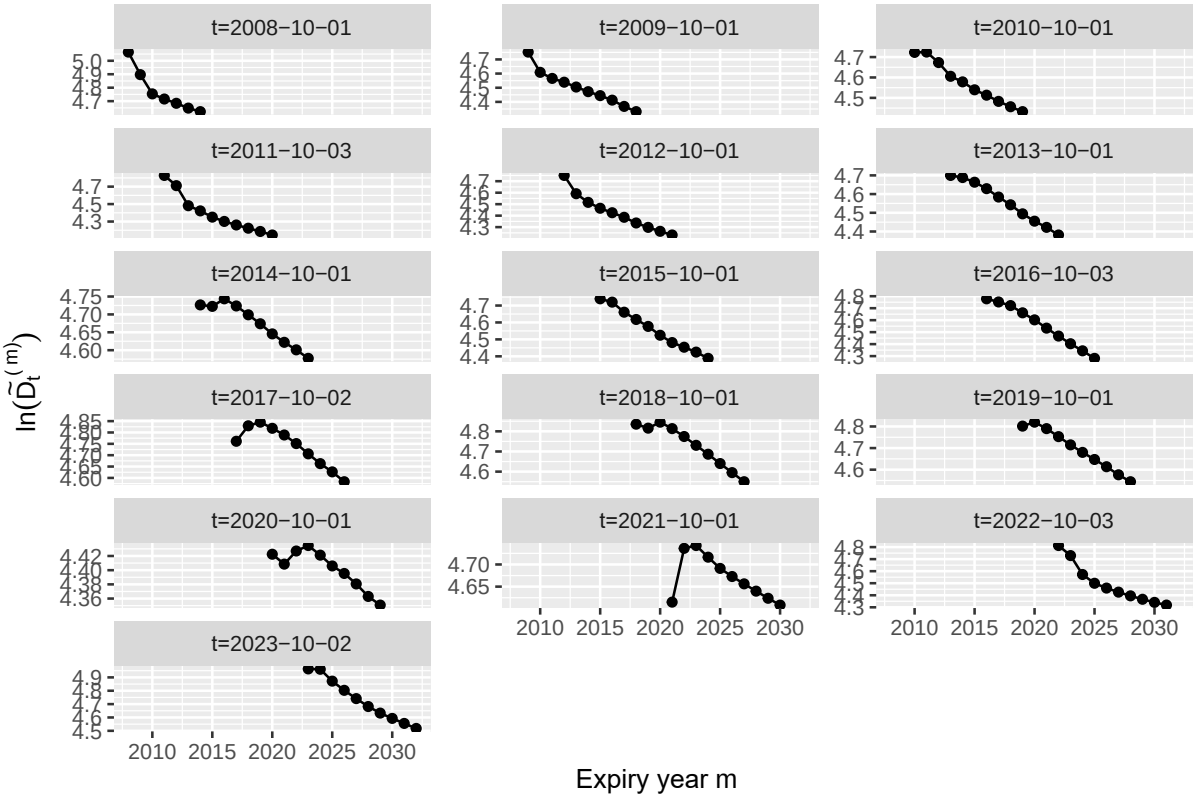

Figure 4: Logarithm of discounted maturity curves

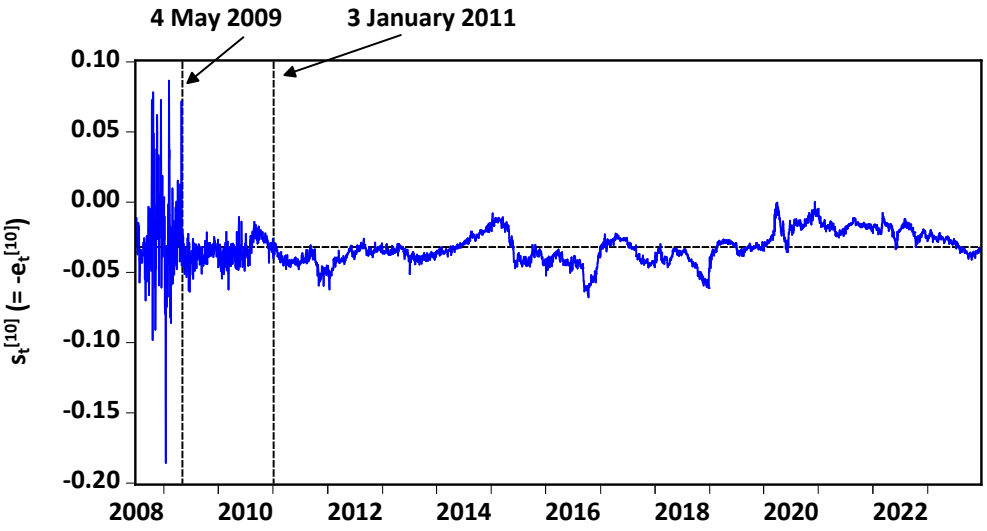

Figure 5: Slope of discounted maturity curves for 10-year dividend futures

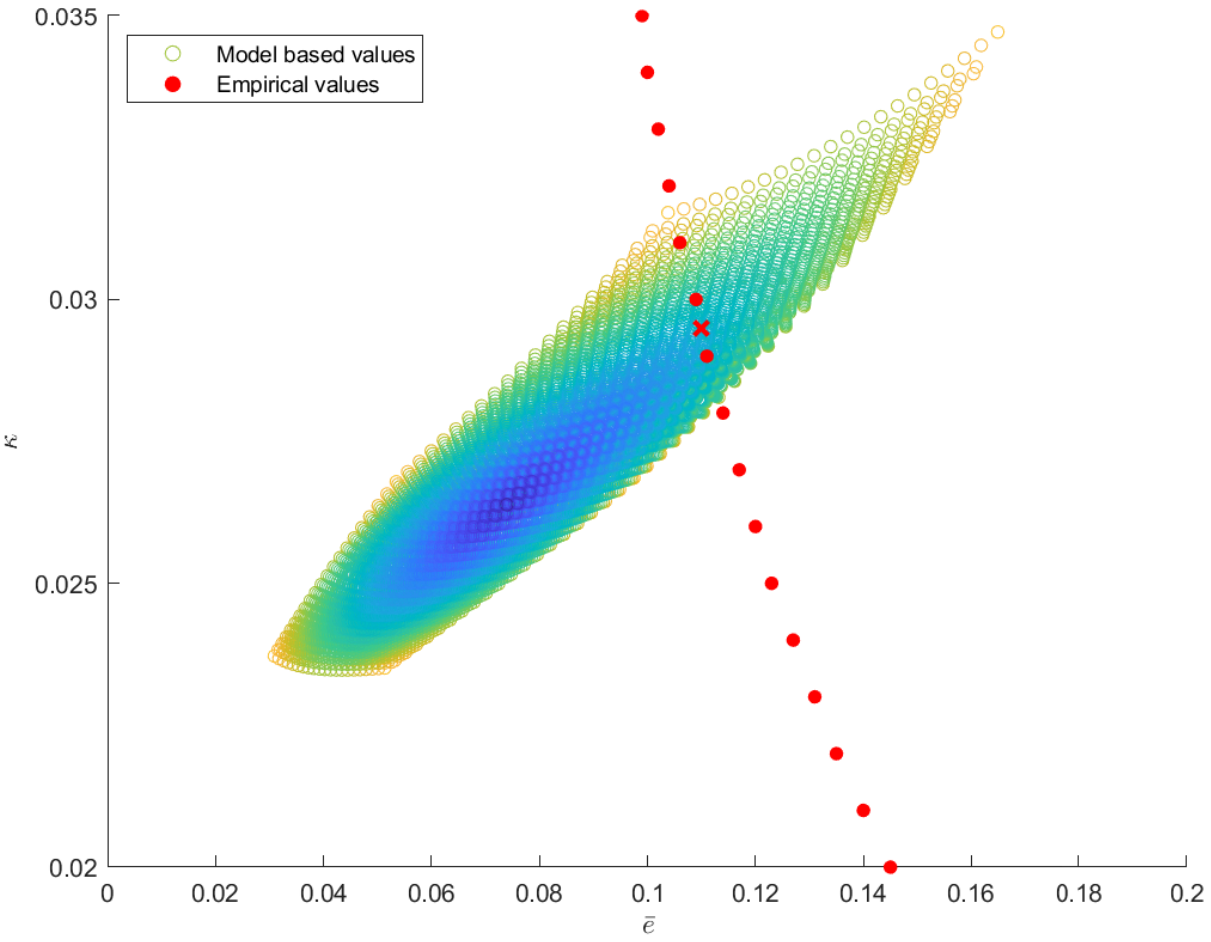

Figure 6: Forward equity yields of dividend futures

The scatterplot shows the combinations of the limiting forward equity yield $\bar{e}$ and the convergence speed κ for the approximated forward equity yield curve from the long-run risk model. The benchmark parameters, taken from Bansal et al. (2016), are given in Table 1. We vary the mean reversion speeds ρ_x, ρ_v and the volatilities σ_x, σ_v by up to $\pm$ standard errors. The deviation of the parameters from the benchmark is largest for the yellow points, and smallest for the blue points. The red dots refer to our empirical data. They represent $(\kappa, \bar{e})$-combinations, for which the (empircally) extracted bubble is positive at all points.

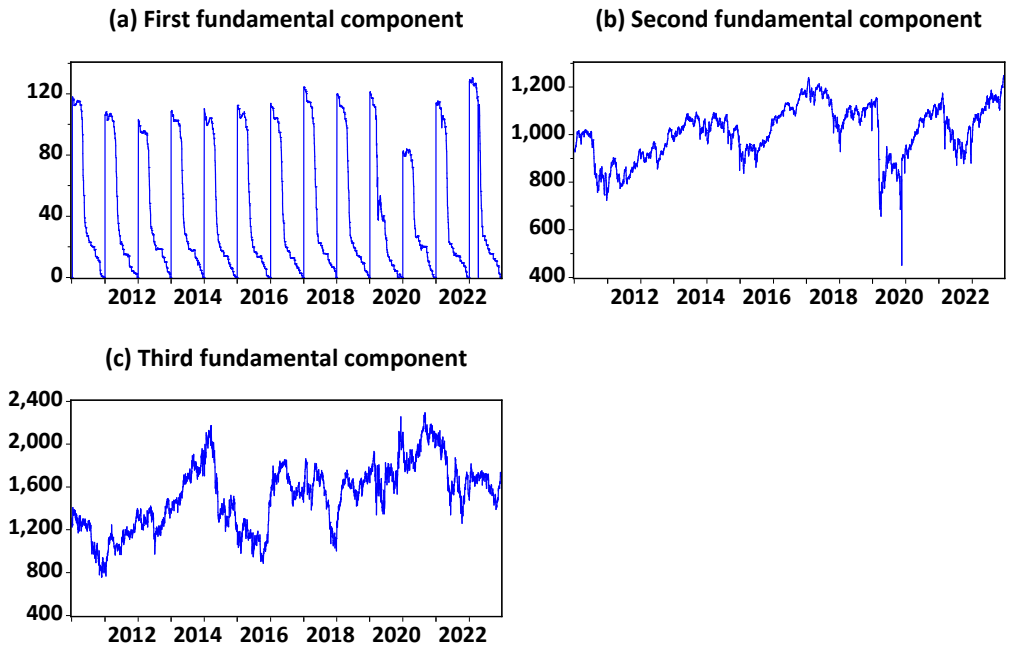

Figure 7: Fundamental components (a) fv_{1t}, (b) fv_{2t}, (c) fv_{3t} under the parameters $\kappa = 0.0295, \bar{e} = -\bar{s}^{[\infty]} = 0.11$.

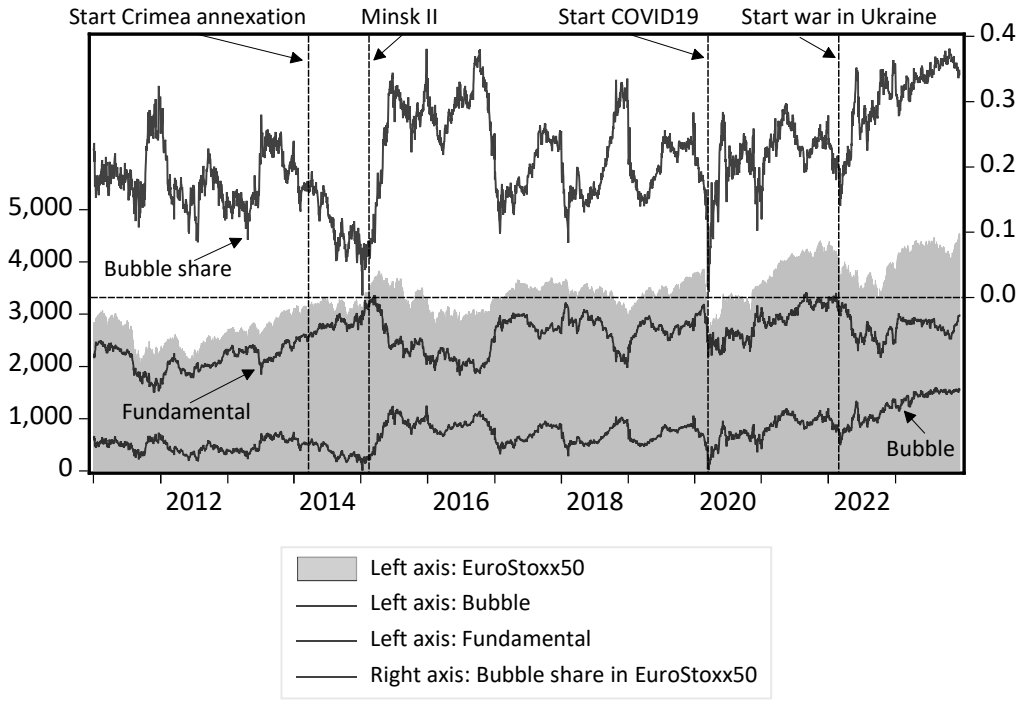

Figure 8: EuroStoxx50 (P_t), fundamental (P_t^f), bubble (B_t), and bubble share in EuroStoxx50 ($= B_t/P_t$).

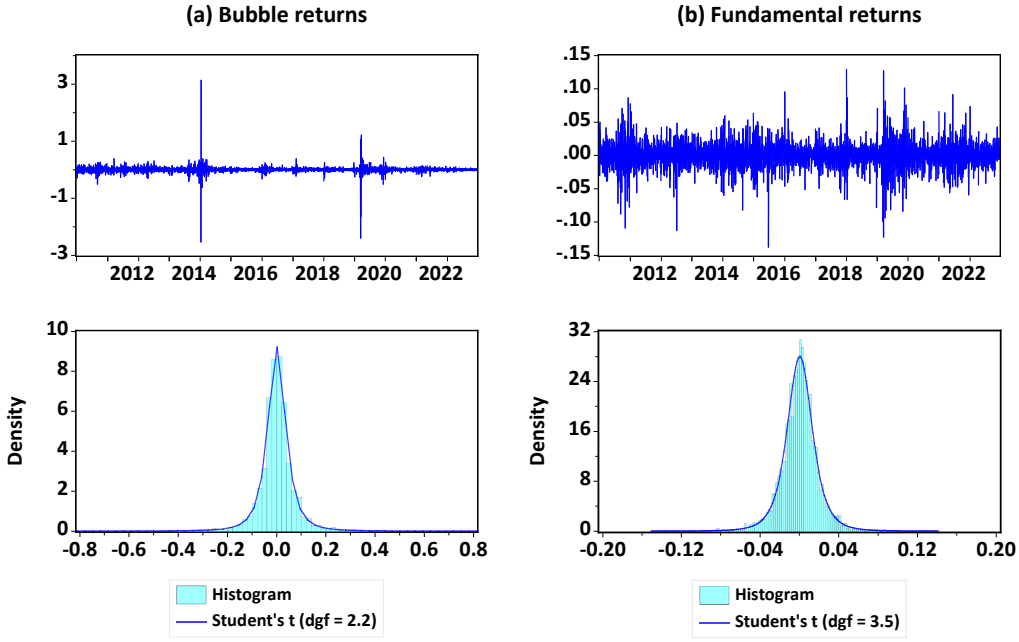

Figure 9: Daily bubble and fundamtental returns along with histograms and fitted t-distributions.

Online Appendix

Online Appendix

B Long-run risk model

B.1 Model setup

We consider a long-run risk model, following Bansal and Yaron (2004), with stochastic expected growth and stochastic volatility. The dynamics of aggregate consumption are

$$\Delta \ln C_{t+1} = (\mu_c + x_t)dt + \sigma_c \sqrt{V_t}\epsilon_{c,t+1} \tag{B.1}$$

where the expected growth rate x and the local variance V are given by

$$\begin{aligned} x_{t+1} &= \rho_x x_t + \sigma_x \sqrt{V_t}\epsilon_{x,t+1} && \text{(B.2)} \\ V_{t+1} &= (1-\rho_v)\bar{V} + \rho_v V_t + \sigma_v \epsilon_{v,t+1} && \text{(B.3)} \end{aligned}$$

ϵ_c, ϵ_x, and ϵ_v are independent standard normally distributed random variables.

The representative investor has Epstein-Zin preferences with relative risk aversion γ and intertemporal elasticity of substitution ψ. We assume $\gamma, \psi > 1$, which implies a preference for early resolution of uncertainty. We set $\theta = \frac{1-\gamma}{1-\frac{1}{\psi}}$.

The log pricing kernel m is given by

$$m_{t+1} = \theta \ln \delta - \frac{\theta}{\psi}\Delta \ln C_{t+1} - (1-\theta)\ln R_{c,t+1} \tag{B.4}$$

where $R_{c,t+1}$ is the return on the consumption claim. We rely on the Campbell-Shiller approximation

$$\ln R_{c,t+1} = \kappa_{c,0} + \kappa_{c,1} w_{t+1} - w_t + \Delta \ln C_{t+1} \tag{B.5}$$

where w is the log price-consumption ratio. The linearization coefficients $\kappa_{c,0}$ and $\kappa_{c,1}$ are given by

$$\begin{aligned} \kappa_{c,0} &= -\kappa_{c,1}\ln \kappa_{c,1} - (1-\kappa_{c,1})\ln(1-\kappa_{c,1}) && \text{(B.6)} \\ \kappa_{c,1} &= \frac{e^{E[w]}}{1+e^{E[w]}} && \text{(B.7)} \end{aligned}$$

For w, we rely on the affine guess $w_t = A_{c,0} + A_{c,x}x_t + A_{c,v}V_t$.

B.2 Consumption Claim

The consumption claim has to meet the Euler equation

$$E\left[e^{m_{t+1}+\ln R_{c,t+1}}\right] = 1 \tag{B.8}$$

Plugging the Campbell-Shiller approximation for the return into the exponent yields

$$
\begin{aligned}
& m_{t+1} + \ln R_{c,t+1} && \text{(B.9)}\\
&= \theta \ln \delta - \frac{\theta}{\psi}\Delta \ln C_{t+1} + \theta \ln R_{c,t+1} && \text{(B.10)}\\
&= \theta \ln \delta - \frac{\theta}{\psi}\Delta \ln C_{t+1} + \theta\kappa_{c,0} + \theta\kappa_{c,1} w_{t+1} - \theta w_t + \theta\Delta \ln C_{t+1} && \text{(B.11)}\\
&= \theta \ln \delta + (1-\gamma)\Delta \ln C_{t+1} + \theta\kappa_{c,0} + \theta\kappa_{c,1} w_{t+1} - \theta w_t && \text{(B.12)}
\end{aligned}
$$

With the linear guess for w and the dynamics of the state variables, this gives

$$
\begin{aligned}
& m_{t+1} + \ln R_{c,t+1} && \text{(B.13)}\\
&= \theta \ln \delta + (1-\gamma)\Delta \ln C_{t+1} + \theta\kappa_{c,0} + \theta\kappa_{c,1} w_{t+1} - \theta w_t && \text{(B.14)}\\
&= \theta \ln \delta + (1-\gamma)\left[\mu_c + x_t + \sigma_c\sqrt{V_t}\epsilon_{c,t+1}\right] + \theta\kappa_{c,0}\\
&\quad + \theta\kappa_{c,1}\left[A_{c,0} + A_{c,x}\left(\rho_x x_t + \sigma_x\sqrt{V_t}\epsilon_{x,t+1}\right) + A_{c,V}\left((1-\rho_v)\bar{V} + \rho_v V_t + \sigma_v\epsilon_{v,t}\right)\right]\\
&\quad - \theta\left[A_{c,0} + A_{c,x}x_t + A_{c,V}V_t\right] && \text{(B.15)}
\end{aligned}
$$

Plugging into the Euler equation and calculating the expectation gives

$$
\begin{aligned}
\theta \ln \delta + (1-\gamma)\mu_c + (1-\gamma)x_t + 0.5(1-\gamma)^2\sigma_c^2 V_t + \theta\kappa_{c,0}&\\
+ \theta\kappa_{c,1}A_{c,0} + \theta\kappa_{c,1}A_{c,x}\rho_x x_t + 0.5\theta^2\kappa_{c,1}^2 A_{c,x}^2\sigma_x^2 V_t&\\
+ \theta\kappa_{c,1}A_{c,V}(1-\rho_v)\bar{V} + \theta\kappa_{c,1}A_{c,V}\rho_v V_t + 0.5\theta^2\kappa_{c,1}^2 A_{c,V}^2\sigma_v^2&\\
- \theta A_{c,0} - \theta A_{c,x}x_t - \theta A_{c,V}V_t &= 0 \qquad \text{(B.16)}
\end{aligned}
$$

Sorting terms gives

$$
\begin{aligned}
\theta \ln \delta + (1-\gamma)\mu_c + \theta\kappa_{c,0} + \theta\kappa_{c,1}A_{c,0} && \text{(B.17)}\\
+ \theta\kappa_{c,1}A_{c,V}(1-\rho_v)\bar{V} + 0.5\theta^2\kappa_{c,1}^2 A_{c,V}^2\sigma_v^2 - \theta A_{c,0} &= 0 && \text{(B.18)}\\
(1-\gamma) + \theta\kappa_{c,1}A_{c,x}\rho_x - \theta A_{c,x} &= 0 && \text{(B.19)}\\
0.5(1-\gamma)^2\sigma_c^2 + 0.5\theta^2\kappa_{c,1}^2 A_{c,x}^2\sigma_x^2 + \theta\kappa_{c,1}A_{c,V}\rho_v - \theta A_{c,V} &= 0 && \text{(B.20)}
\end{aligned}
$$

Solving for the coefficients gives

$$
\begin{aligned}
A_{c,0} &= \frac{\ln\delta + \left(1-\frac{1}{\psi}\right)\mu_c + \kappa_{c,0} + \kappa_{c,1}A_{c,V}(1-\rho_v)\bar{V} + 0.5\theta\kappa_{c,1}^2 A_{c,V}^2\sigma_v^2}{1-\kappa_{c,1}} && \text{(B.21)}\\
A_{c,x} &= \frac{1-\frac{1}{\psi}}{1-\kappa_{c,1}\rho_x} && \text{(B.22)}\\
A_{c,V} &= \frac{0.5(1-\gamma)\left(1-\frac{1}{\psi}\right)\sigma_c^2 + 0.5\theta\kappa_{c,1}^2 A_{c,x}^2\sigma_x^2}{1-\kappa_{c,1}\rho_v} && \text{(B.23)}
\end{aligned}
$$

B.3 Stochastic discount factor

The stochastic discount factor can thus be written as

$$
\begin{aligned}
& m_{t+1} \\
&= \theta \ln \delta - \frac{\theta}{\psi} \Delta \ln C_{t+1} + (\theta - 1) \ln R_{c,t+1} \\
&= \theta \ln \delta - \frac{\theta}{\psi} \Delta \ln C_{t+1} + (\theta - 1) \left[\kappa_{c,0} + \kappa_{c,1} w_{t+1} - w_t + \Delta \ln C_{t+1} \right] \\
&= \theta \ln \delta - \gamma \Delta \ln C_{t+1} + (\theta - 1)\kappa_{c,0} + (\theta - 1)\kappa_{c,1} w_{t+1} - (\theta - 1) w_t \\
&= \theta \ln \delta - \gamma \mu_C - \gamma x_t - \gamma \sigma_c \sqrt{V_t} \epsilon_{c,t+1} + (\theta - 1)\kappa_{c,0} \\
&\quad + (\theta - 1)\kappa_{c,1} A_{c,0} + (\theta - 1)\kappa_{c,1} A_{c,x} \left[\rho_x x_t + \sigma_x \sqrt{V_t} \epsilon_{x,t+1} \right] \\
&\quad + (\theta - 1)\kappa_{c,1} A_{c,V} \left[(1 - \rho_v) \bar{V} + \rho_v V_t + \sigma_v \epsilon_{v,t+1} \right] \\
&\quad - (\theta - 1) A_{c,0} - (\theta - 1) A_{c,x} x_t - (\theta - 1) A_{c,V} V_t \\
&= \theta \ln \delta - \gamma \mu_C - \gamma x_t - \gamma \sigma_c \sqrt{V_t} \epsilon_{c,t+1} + (\theta - 1)\kappa_{c,0} \\
&\quad + (\theta - 1)\kappa_{c,1} A_{c,0} + (\theta - 1)\kappa_{c,1} A_{c,x} \left[\rho_x x_t + \sigma_x \sqrt{V_t} \epsilon_{x,t+1} \right] \\
&\quad + (\theta - 1)\kappa_{c,1} A_{c,V} \left[(1 - \rho_v) \bar{V} + \rho_v V_t + \sigma_v \epsilon_{v,t+1} \right] \\
&\quad - (\theta - 1) A_{c,0} - (\theta - 1) A_{c,x} x_t - (\theta - 1) A_{c,V} V_t \qquad \text{(B.24)} \\
&= \theta \ln \delta - \gamma \mu_C + (\theta - 1)\kappa_{c,0} - (\theta - 1)(1 - \kappa_{c,1}) A_{c,0} + (\theta - 1)\kappa_{c,1} A_{c,V} (1 - \rho_v) \bar{V} \\
&\quad + \left[(\theta - 1)\kappa_{c,1} A_{c,x} \rho_x - (\theta - 1) A_{c,x} - \gamma \right] x_t \\
&\quad + \left[(\theta - 1)\kappa_{c,1} A_{c,V} \rho_v - (\theta - 1) A_{c,V} \right] V_t \\
&\quad - \gamma \sigma_c \sqrt{V_t} \epsilon_{c,t+1} - (1 - \theta)\kappa_{c,1} A_{c,x} \sigma_x \sqrt{V_t} \epsilon_{x,t+1} - (1 - \theta)\kappa_{c,1} A_{c,V} \\
&\quad - (\theta - 1) A_{c,0} - (\theta - 1) A_{c,x} x_t - (\theta - 1) A_{c,V} V_t \qquad \text{(B.25)} \\
&= \theta \ln \delta - \gamma \mu_C + (\theta - 1)\kappa_{c,0} - (\theta - 1)(1 - \kappa_{c,1}) A_{c,0} + (\theta - 1)\kappa_{c,1} A_{c,V} (1 - \rho_v) \bar{V} \\
&\quad + \left[(1 - \theta)(1 - \kappa_{c,1} \rho_x) A_{c,x} - \gamma \right] x_t + (1 - \theta)(1 - \kappa_{c,1} \rho_v) A_{c,V} V_t \\
&\quad - \gamma \sigma_c \sqrt{V_t} \epsilon_{c,t+1} - (1 - \theta)\kappa_{c,1} A_{c,x} \sigma_x \sqrt{V_t} \epsilon_{x,t+1} - (1 - \theta)\kappa_{c,1} A_{c,V} \sigma_v \epsilon_{v,t+1} \qquad \text{(B.26)}
\end{aligned}
$$

In the following, we abbreviate m_{t+1} as

$$
m_{t+1} = m_0 + m_x x_t + m_v V_t - \lambda_c \sqrt{V_t} \epsilon_{c,t+1} - \lambda_x \sqrt{V_t} \epsilon_{x,t+1} - \lambda_v \epsilon_{v,t+1} \qquad \text{(B.27)}
$$

where

$$
\begin{aligned}
m_0 &= \theta \ln \delta - \gamma \mu_C + (\theta - 1)\kappa_{c,0} - (\theta - 1)(1 - \kappa_{c,1}) A_{c,0} + (\theta - 1)\kappa_{c,1} A_{c,V} (1 - \rho_v) \bar{V} \\
m_x &= (1 - \theta)(1 - \kappa_{c,1} \rho_x) A_{c,x} - \gamma \\
m_v &= (1 - \theta)(1 - \kappa_{c,1} \rho_v) A_{c,V} \qquad \text{(B.28)}
\end{aligned}
$$

and where the market prices of risk are

$$\begin{aligned}\lambda_c &= \gamma\sigma_c \\ \lambda_x &= (1-\theta)\kappa_{c,1}A_{c,x}\sigma_x \\ \lambda_v &= (1-\theta)\kappa_{c,1}A_{c,V}\sigma_v\end{aligned}$$

B.4 Dividend Claim

The dynamics of the dividends are given by

$$\Delta \ln D_{t+1} = \mu_d + \phi_d x_t + \sigma_{dc}\sqrt{V_t}\epsilon_{c,t+1} + \sigma_{dd}\sqrt{V_t}\epsilon_{d,t+1} \tag{B.29}$$

The dividend claim has to meet the Euler equation

$$E\left[e^{m_{t+1}+\ln R_{d,t+1}}\right] = 1 \tag{B.30}$$

With the Campbell-Shiller approximation for the return, the linear guess for the log price-dividend ratio w_d, and the dynamics of the state variables, this gives

$$m_{t+1} + \ln R_{d,t+1} \tag{B.31}$$

$$\begin{aligned}&= m_0 + m_x x_t + m_v V_t - \lambda_c\sqrt{V_t}\epsilon_{c,t+1} - \lambda_x\sqrt{V_t}\epsilon_{x,t+1} - \lambda_v\epsilon_{v,t+1} \\ &\quad + \kappa_{d,0} + \kappa_{d,1}w_{d,t+1} - w_{d,t} + \Delta \ln D_{t+1}\end{aligned} \tag{B.32}$$

$$\begin{aligned}&= m_0 + m_x x_t + m_v V_t - \lambda_c\sqrt{V_t}\epsilon_{c,t+1} - \lambda_x\sqrt{V_t}\epsilon_{x,t+1} - \lambda_v\epsilon_{v,t+1} \\ &\quad + \kappa_{d,0} + \kappa_{d,1}\left[A_{d,0} + A_{d,x}\left(\rho_x x_t + \sigma_x\sqrt{V_t}\epsilon_{x,t+1}\right) + A_{d,V}\left((1-\rho_v)\bar{V} + \rho_v V_t + \sigma_v\epsilon_{v,t}\right)\right] \\ &\quad - \left[A_{d,0} + A_{d,x}x_t + A_{d,V}V_t\right] \\ &\quad + \mu_d + \phi_d x_t + \sigma_{dc}\sqrt{V_t}\epsilon_{c,t+1} + \sigma_{dd}\sqrt{V_t}\epsilon_{d,t+1}\end{aligned} \tag{B.33}$$

$$\begin{aligned}&= m_0 + \kappa_{d,0} + \kappa_{d,1}A_{d,0} + \kappa_{d,1}A_{d,V}(1-\rho_v)\bar{V} - A_{d,0} + \mu_d \\ &\quad + \left[m_x + \kappa_{d,1}A_{d,x}\rho_x - A_{d,x} + \phi_d\right]x_t + \left[m_v + \kappa_{d,1}A_{d,v}\rho_v - A_{d,v}\right]V_t \\ &\quad + \left(\sigma_{dc} - \lambda_c\right)\sqrt{V_t}\epsilon_{c,t+1} + \left(\kappa_{d,1}A_{d,x}\sigma_x - \lambda_x\right)\sqrt{V_t}\epsilon_{x,t+1} \\ &\quad + \left(\kappa_{d,1}A_{d,v}\sigma_v - \lambda_v\right)\epsilon_{v,t+1} + \sigma_{dd}\sqrt{V_t}\epsilon_{d,t+1}\end{aligned} \tag{B.34}$$

Plugging into the Euler equation and calculating the expectation gives

$$\begin{aligned}&m_0 + \kappa_{d,0} - (1-\kappa_{d,1})A_{d,0} + \kappa_{d,1}A_{d,V}(1-\rho_v)\bar{V} + \mu_d \\ &+\left[m_x - (1-\kappa_{d,1}\rho_x)A_{d,x} + \phi_d\right]x_t + \left[m_v - (1-\kappa_{d,1}\rho_v)A_{d,v}\right]V_t \\ &+0.5\left(\sigma_{dc} - \lambda_c\right)^2 V_t + 0.5\left(\kappa_{d,1}A_{d,x}\sigma_x - \lambda_x\right)^2 V_t \\ &+0.5\left(\kappa_{d,1}A_{d,v}\sigma_v - \lambda_v\right)^2 + 0.5\sigma_{dd}^2 V_t = 0\end{aligned} \tag{B.35}$$

Sorting terms gives

$$m_0 + \kappa_{d,0} - (1-\kappa_{d,1})A_{d,0} + \kappa_{d,1}A_{d,V}(1-\rho_v)\bar{V} + \mu_d + 0.5\left(\kappa_{d,1}A_{d,v}\sigma_v - \lambda_v\right)^2 = 0 \quad \text{(B.36)}$$

$$m_x - (1-\kappa_{d,1}\rho_x)A_{d,x} + \phi_d = 0 \quad \text{(B.37)}$$

$$m_v - (1-\kappa_{d,1}\rho_v)A_{d,v} + 0.5\left(\sigma_{dc} - \lambda_c\right)^2 + 0.5\left(\kappa_{d,1}A_{d,x}\sigma_x - \lambda_x\right)^2 + 0.5\sigma_{dd}^2 = 0 \quad \text{(B.38)}$$

Solving for the coefficients gives

$$A_{d,0} = \frac{m_0 + \kappa_{d,0} + \kappa_{d,1}A_{d,V}(1-\rho_v)\bar{V} + \mu_d + 0.5\left(\kappa_{d,1}A_{d,v}\sigma_v - \lambda_v\right)^2}{1-\kappa_{d,1}} \quad \text{(B.39)}$$

$$A_{d,x} = \frac{m_x + \phi_d}{1-\kappa_{d,1}\rho_x} \quad \text{(B.40)}$$

$$A_{d,V} = \frac{m_v + 0.5\left(\sigma_{dc} - \lambda_c\right)^2 + 0.5\left(\kappa_{d,1}A_{d,x}\sigma_x - \lambda_x\right)^2 + 0.5\sigma_{dd}^2}{1-\kappa_{d,1}\rho_v} \quad \text{(B.41)}$$

B.5 Dividend Strips

The price of the dividend strips follows recursively. For the first dividend claim, we obtain

$$DS_t^{t+1} = D_t\mathbb{E}_t\left[e^{m_{t+1}+\Delta\ln D_{t+1}}\right] \quad \text{(B.42)}$$

$$= D_t e^{m_0+m_x x_t+m_v V_t+\mu_d+\phi_d x_t+0.5(\sigma_{dc}-\lambda_c)^2 V_t+0.5(-\lambda_x)^2 V_t+0.5(-\lambda_v)^2+0.5(\sigma_{dd})^2 V_t} \quad \text{(B.43)}$$

$$= D_t e^{ds_0^1+ds_x^1 x_t+ds_v^1 V_t} \quad \text{(B.44)}$$

where

$$ds_0^1 = m_0 + \mu_d + 0.5(-\lambda_v)^2 \quad \text{(B.45)}$$

$$ds_x^1 = m_x + \phi_d \quad \text{(B.46)}$$

$$ds_v^1 = m_v + 0.5(\sigma_{dc} - \lambda_c)^2 + 0.5(-\lambda_x)^2 + 0.5(\sigma_{dd})^2 \quad \text{(B.47)}$$

For the $(n+1)$st dividend claim, we obtain

$$DS_t^{t+n+1} = \mathbb{E}_t\left[e^{m_{t+1}}DS_{t+1}^{t+n+1}\right] \quad \text{(B.48)}$$

$$= D_t\mathbb{E}_t\left[e^{m_{t+1}+\Delta\ln D_{t+1}+ds_0^n+ds_x^n x_{t+1}+ds_v^n V_{t+1}}\right] \quad \text{(B.49)}$$

$$= D_t e^{ds_0^{n+1}+ds_x^{n+1}x_t+ds_v^{n+1}V_t} \quad \text{(B.50)}$$

where

$$ds_0^{n+1} = m_0 + \mu_d + ds_0^n + ds_v^n(1-\rho_v)\bar{V} + 0.5(ds_v^n\sigma_v - \lambda_v)^2 \quad \text{(B.51)}$$

$$ds_x^{n+1} = m_x + \phi_d + ds_x^n\rho_x \quad \text{(B.52)}$$

$$ds_v^{n+1} = m_v + ds_v^n\rho_v + 0.5(\sigma_{dc} - \lambda_c)^2 + 0.5(ds_x^n\sigma_x - \lambda_x)^2 + 0.5(\sigma_{dd})^2 \quad \text{(B.53)}$$

The limiting values for $n \to \infty$ are

$$\lim_{n\to\infty} ds_0^{n+t} - ds_0^n = m_0 + \mu_d + ds_v^\infty(1-\rho_v)\bar{V} + 0.5(ds_v^\infty\sigma_v - \lambda_v)^2 \tag{B.54}$$

$$\lim_{n\to\infty} ds_x^n = \frac{m_x + \phi_d}{1-\rho_x} \tag{B.55}$$

$$\lim_{n\to\infty} ds_v^n = \frac{m_v + 0.5(\sigma_d - \lambda_c)^2 + 0.5(ds_x^\infty\sigma_x - \lambda_x)^2 + 0.5(\sigma_{dd})^2}{1-\rho_v} \tag{B.56}$$

The term $\lim_{n\to\infty} ds_0^{n+t} - ds_0^n$ is the limiting slope of the log dividend price curve.

We can now write

$$ds_0^{n+1} - ds_0^n \tag{B.57}$$

$$= m_0 + \mu_d + ds_v^\infty(1-\rho_v)\bar{V} + 0.5(ds_v^\infty\sigma_v - \lambda_v)^2 \tag{B.58}$$
$$- ds_v^\infty(1-\rho_v)\bar{V} - 0.5(ds_v^\infty\sigma_v - \lambda_v)^2 + ds_v^n(1-\rho_v)\bar{V} + 0.5(ds_v^n\sigma_v - \lambda_v)^2$$

$$= m_0 + \mu_d + ds_v^\infty(1-\rho_v)\bar{V} + 0.5(ds_v^\infty\sigma_v - \lambda_v)^2 \tag{B.59}$$
$$+ (ds_v^n - ds_v^\infty)(1-\rho_v)\bar{V} + 0.5\left(\sigma_v^2(ds_v^n)^2 - 2\sigma_v ds_v^n\lambda_v - \sigma_v^2(ds_v^\infty)^2 + 2\sigma_v ds_v^\infty\lambda_v\right)$$

$$= m_0 + \mu_d + ds_v^\infty(1-\rho_v)\bar{V} + 0.5(ds_v^\infty\sigma_v - \lambda_v)^2 \tag{B.60}$$
$$+ (ds_v^n - ds_v^\infty)\left[(1-\rho_v)\bar{V} - \sigma_v\lambda_v\right] + 0.5\sigma_v^2\left[(ds_v^n)^2 - (ds_v^\infty)^2\right]$$